SACLANTCEN REPORT
serial no: SR-305

SACLANT UNDERSEA RESEARCH CENTRE REPORT

OCEANOGRAPHIC MEASUREMENTS OF THE WEST BLACK SEA: JUNE 15 TO JULY 5, 1996

D. Di Iorio, T. Akal, P. Guerrini, H. Yüce
E. Gezgin, E. Özsoy

April 1999

The SACLANT Undersea Research Centre provides the Supreme Allied Commander Atlantic (SACLANT) with scientific and technical assistance under the terms of its NATO charter, which entered into force on 1 February 1963. Without prejudice to this main task – and under the policy direction of SACLANT – the Centre also renders scientific and technical assistance to the individual NATO nations.

Oceanographic Measurements of the West Black Sea: June 15 to July 5, 1996

D. Di Iorio, T. Akal, P. Guerrini,
H. Yüce, E. Gezgin, E. Özsoy

The content of this document pertains to work performed under Project 022-1 of the SACLANTCEN Programme of Work. The document has been approved for release by The Director, SACLANTCEN.

Jan L. Spoelstra
Director

intentionally blank page

Oceanographic Measurements of the West Black Sea: June 15 to July 5, 1996

D. Di Iorio, T. Akal, P. Guerrini,
H. Yüce†, E. Gezgin‡, E. Özsoy*

Executive Summary:

This report describes the oceanographic measurement program carried out as part of SACLANTCEN's Black Sea 1996 project in collaboration with the Turkish Navy Department of Navigation, Hydrography and Oceanography. The experimental program was designed to assess the effects of the environment on the performance of operational sonar equipment, mainly those used for ASW. The experimental program was also designed to determine the oceanographic variability, water exchange, water mass formation, spreading and coupling to basin and sub-basin scale circulation. This report concerns itself with the latter. The data described in this report consists of detailed bathymetry from swath mapping which adds to the 1995 measurements, high frequency echo sounder imaging and conductivity-temperature-depth (CTD) profiling for locating the major canyons which transport Mediterranean water to the continental slope. Moored instrumentation recorded detailed Mediterranean inflow characteristics showing that the flow was continuous during the June-July 1996 experimental period. Mediterranean Sea water flowing into the Black Sea forms a thin dense layer on the Black Sea continental shelf. The sound speed characteristics of this thin layer are such that the sea bottom can be masked. This localized effect of masking the sea bottom for a range of acoustic propagation angles may affect propagation loss and reverberation modelling. Also, this masking effect of the sea bottom may affect the detection of underwater objects on the sea floor. Further work in this area consists of comparing oceanographic measurements of the Mediterranean inflow to hydraulic control models so as to be able to predict the characteristics of the Mediterranean water on the continental shelf.

† Eng. Capt., Assoc. Prof. Dr. Hüseyin Yüce, TUNA
Turkish National Representative, SACLANTCEN
Scientific Committee of National Representatives,
Head, Department of Navigation, Hydrography and Oceanography,
Istanbul, Turkey
‡ Lt. Erhan Gezgin,
Department of Navigation, Hydrography and Oceanography,
Istanbul, Turkey
* Dr. Emin Özsoy,
Institute of Marine Sciences,
Erdemli, Turkey

intentionally blank page

Oceanographic Measurements of the West Black Sea: June 15 to July 5, 1996

D. Di Iorio, T. Akal, P. Guerrini, H. Yüce,
E. Gezgin, E. Özsoy

Abstract:

An extensive survey was carried out in the Black Sea exit region of the Strait of Istanbul (Bosporus). The data described in this report builds on the knowledge learned during the Black Sea 1995 sea trial. Extensive measurements were made at the northern sill so as to describe the internal hydraulic conditions. It is shown that flow over the sill at three measurement points (south of the sill, on the sill and north of the sill) is subcritical. During the observation period the flow of Mediterranean water was continuous (i.e. no blockage events occurred as the relative sea level difference did not exceed 45 cm). The Mediterranean bottom boundary layer showed strong levels of turbulence and measurements of bottom friction coefficient ranged from 5 to 15 $\times$ 10^{-3}.

The flow of Mediterranean water on the continental shelf is subcritical and the dilution occurs at a rate of 0.1 psu km^{-1}. Echo sounder imaging identified the major canyons which carry the effluent out to the continental slope. During the shelf survey a cyclonic circulation pattern was observed and during the deep sea survey the circulation pattern showed a general eastward direction with possibly a Rossby wave instability of approximately 70 km in wavelength. NOAA satellite infrared images could not be used to reveal such instabilities.

Contents

List of Figures

List of Tables

intentionally blank page

1

Introduction

The West Black June-July 1996 environmental measurements provided an opportunity to continue studying the physical oceanography of the southwestern Black Sea region. The experimental design was devoted to increasing the knowledge learned during the West Black sea trial in 1995 (see Di Iorio and Yüce, 1999), by studying three main areas: the Black Sea exit region, the Black Sea continental shelf region and the continental slope / deep sea region. Figure 1 shows these regions of study with ship tracks superimposed. This survey provides the necessary information for understanding the physical oceanographic processes in this area during this time.

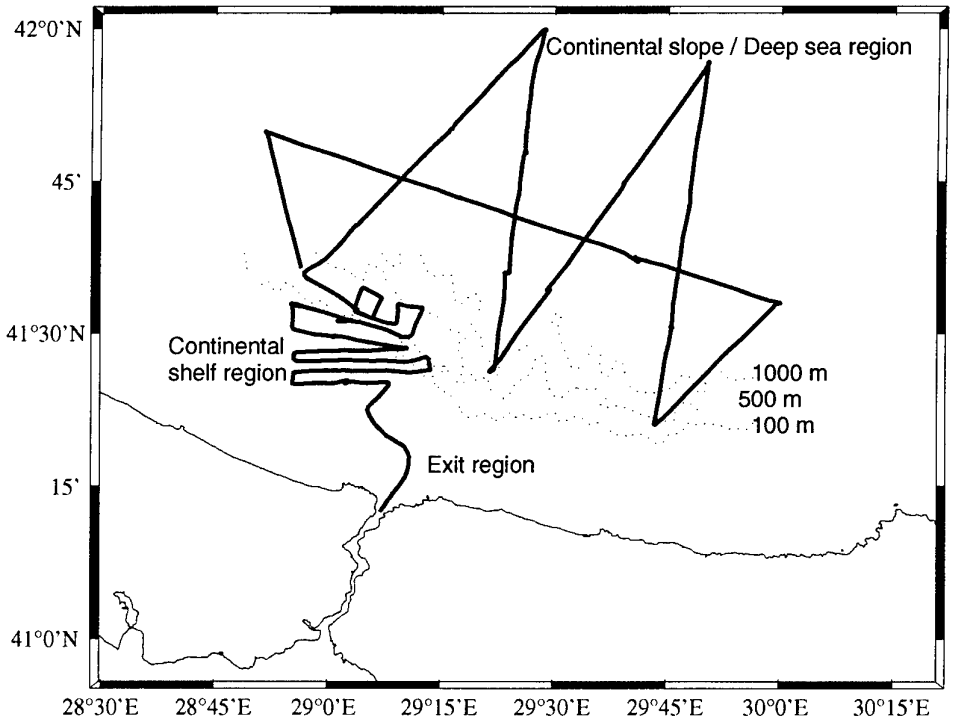

Figure 1 *Three major study areas: the Black Sea exit region, the Black Sea continental shelf region and the continental slope/deep sea region.*

The Black Sea exit region provides a unique opportunity to study the internal hydraulics of sill flows. The northern sill that exists in the Black Sea exit region (3 km northeast of the entrance to the Strait of Istanbul (Bosporus)) acts as a control for Mediterranean flow into the Black Sea. Previous measurements in this area ((Di Iorio and Yüce, 1999)) showed complete but temporary blockage of the Mediterranean flow over time scales of 2-3 days because of meteorological effects thus concluding that the inflow is not always continuous.

The continental shelf region is an area with complex bathymetry. Since the Mediterranean inflow is described as a "delta-like" flow pattern, one of the objectives of this sea trial was to locate the major canyons containing Mediterranean water, measure the dilution and speed, and map its path.

The continental slope / deep sea region is an area of great interest because the Black Sea beyond 150 m is anoxic, containing high levels of hydrogen sulfide (H_2S). An investigation of the current system is made to establish its meandering three dimensional hydrographic structure.

2
Experiment

Oceanographic instrumentation consisting of sea level instruments, current meters, thermistor chains, an acoustic Doppler current profiler (ADCP), an acoustic scintillation instrument and a CTD station were moored in the Strait of Istanbul (Bosporus) and at the exit region of the Black Sea. These instruments are used to monitor the exchange of Black Sea and Mediterranean sea water as well as provide a detailed analysis of the internal hydraulic exchange at the northern sill. This is accomplished with two moorings, each consisting of two current meters and a thermistor chain, placed south and north of the sill and the ADCP mooring placed on the sill. Figure 2 shows a map of the Black Sea exit region showing mooring locations together with the northern sill location; Table 1 lists the location for each.

The sea level stations located at Anadolukavagi and Fenerbahce are used to obtain measurement of the sea level difference between the Black Sea basin and Marmara Sea basin. The locations are the same as those pictured in Di Iorio and Yüce (1999). During the course of this experiment no meteorological data was obtained.

During the Black Sea 1995 experiment, SWATH mapping of the exit region was obtained in order to obtain detailed hydrographic data (Di Iorio and Yüce, 1999). During this 1996 sea trial, SWATH mapping was extended out onto the continental shelf. The bottom bathymetry results from both sea trials are shown in Figure 3.

Instrument	Latitude	Longitude	Depth (m)
Mooring station 1	41° 13.68' N	29° 8.15' E	71
Mooring station 2	41° 15.84' N	29° 10.17' E	87.5
Scintillation transmitter	41° 13.67' N	29° 8.29' E	71
Scintillation receiver	41° 13.80' N	29° 8.09' E	73
ADCP	41° 14.84' N	29° 9.17' E	62
CTD station	41° 14.37' N	29° 8.7' E	63
Sea level (Anadolukavagi)	41° 10.73' N	29° 5.23' E	
Sea level (Fenerbahce)	40° 58.10' N	29° 1.95' E	
Sill location	41° 14.75' N	29° 9.32' E	60

Table 1 *Instrument mooring locations in the Strait of Istanbul and Black Sea exit region.*

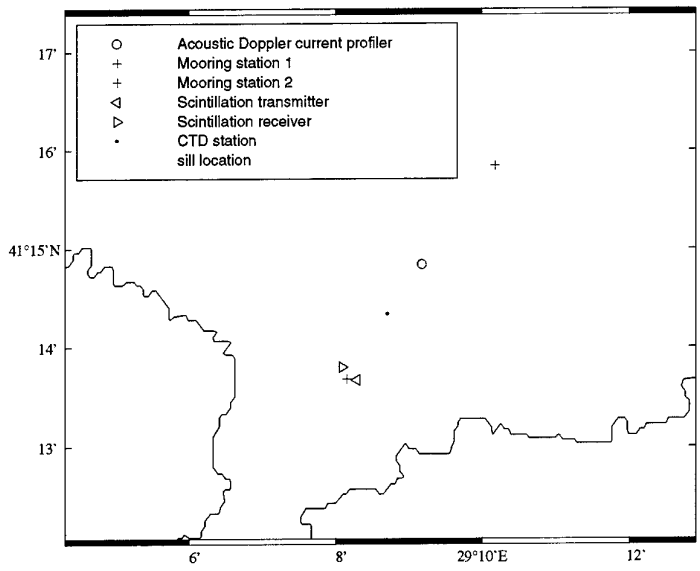

Figure 2 *The Black Sea exit region showing the location of the acoustic Doppler current profiler, the acoustic scintillation transmitter and receiver, two current meter stations and TCG Çubuklu CTD station.*

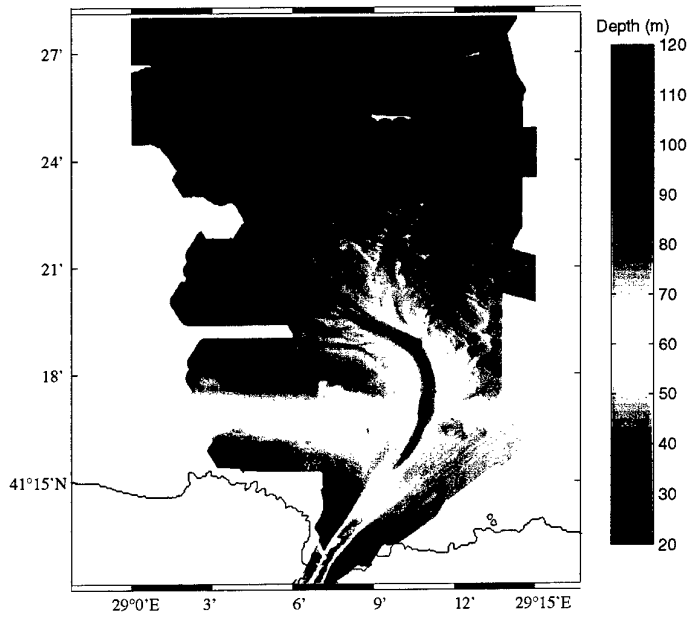

Figure 3 *Bottom bathymetry in the Black Sea exit region using the multi beam SWATH echo sounder.*

The northwestern part of the image shows that there exists a major canyon on the shelf region which is directed in the northwestern direction. The less diluted Mediterranean water is expected to be found within this canyon.

3

Strait of Istanbul (Bosporus) / Black Sea Exit Region

3.1 Sea level data

Sea level data for the measurement period is shown in Figure 4 together with the difference. Much diurnal and semi-diurnal variations exist in the measurement possibly associated with atmospheric pressure changes and small tidal effects. A significant drop in the sea level difference occurs on Julian Day 180 which is due to a significant increase in the sea level at the southern station, Fenerbahce. This may be the result of a lower atmospheric pressure system in the Marmara Sea compared to that in the Black Sea. Ozsoy et al. (1997) document changes in sea level heights which are associated with possible high/low pressure systems set up in the Black Sea.

3.2 Acoustic Doppler current profiler

The acoustic Doppler current profiler was bottom mounted on the sill in the Black Sea exit region. Table 2 lists the relevant set up parameters. The ADCP transmits once every 12 s and obtains a 20 transmission ensemble average every 5 min. Three components of current are obtained: N-S, E-W and vertical at 1 m bin intervals for 50 bins. The physical characteristic of this instrument allow measurement close to the bottom boundary (first sample is 2.2 m from the bottom).

Since the ADCP is moored within a canyon oriented approximately 38° from True North, the component of flow parallel and perpendicular to this direction is calculated and plotted in Figure 5. Positive values correspond to flow toward the North and West for the along and cross stream current component respectively. White is used to denote zero current. During the measurement period the Mediterranean inflow into the Black Sea was continuous. The increase in flow on Julian day 180 seems to be well correlated with the sea level difference showing a minimum. Also the lower Mediterranean flow rate on Julian day 177.5 may be the result of the higher sea level difference.

The cross stream component shows a change from eastward to westward flow for the upper Black Sea layer on Julian day 181 which may be associated with meteorological

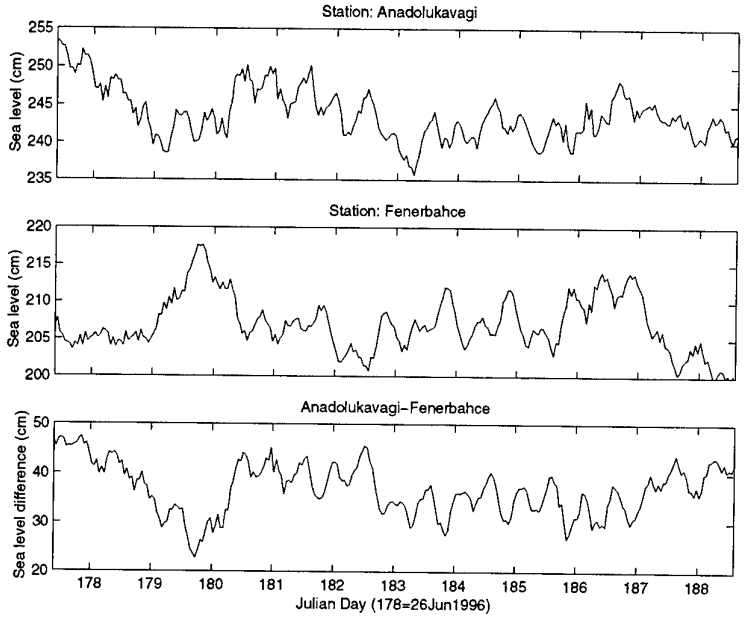

Figure 4 *Sea level data from the northern station Anadolukavagi and the southern station Fenerbahce together with the difference.*

changes. Unfortunately no meteorological data were obtained during the course of the experiment and therefore no direct comparison is possible. It is widely known in the literature that the Black Sea responds very quickly to meteorological changes.

The current shear is shown in Figure 6. It is calculated in 1 m depth intervals with the z-axis positive upwards. Maximum shear observed was $-0.5\ s^{-1}$ in the along stream component. The shear existing in the cross stream component for the lower Mediterranean layer may correspond to a spiraling circulation pattern within the canyon due to bathymetry changes along the canyon.

The Froude number,

$$F^2 = \frac{U^2}{g'h} \tag{1}$$

where U is the mean flow speed resolved along the direction of the canyon, $g' = \Delta\rho/\rho g$ is the reduced gravity and h is the Mediterranean layer thickness, gives a measure of the ratio of kinetic to potential energy. We consider a single layer reduced gravity flow since the Mediterranean layer is confined by the channel whereas the Black Sea layer is not. This dimensionless parameter gives a measure of hydraulic control ($F^2 = 1$) at a sill crest which separates subcritical and supercritical flow. For supercritical flow ($F^2 > 1$), the kinetic energy exceeds the potential energy and a hydraulic jump occurs which results in intense turbulence and so entrainment and

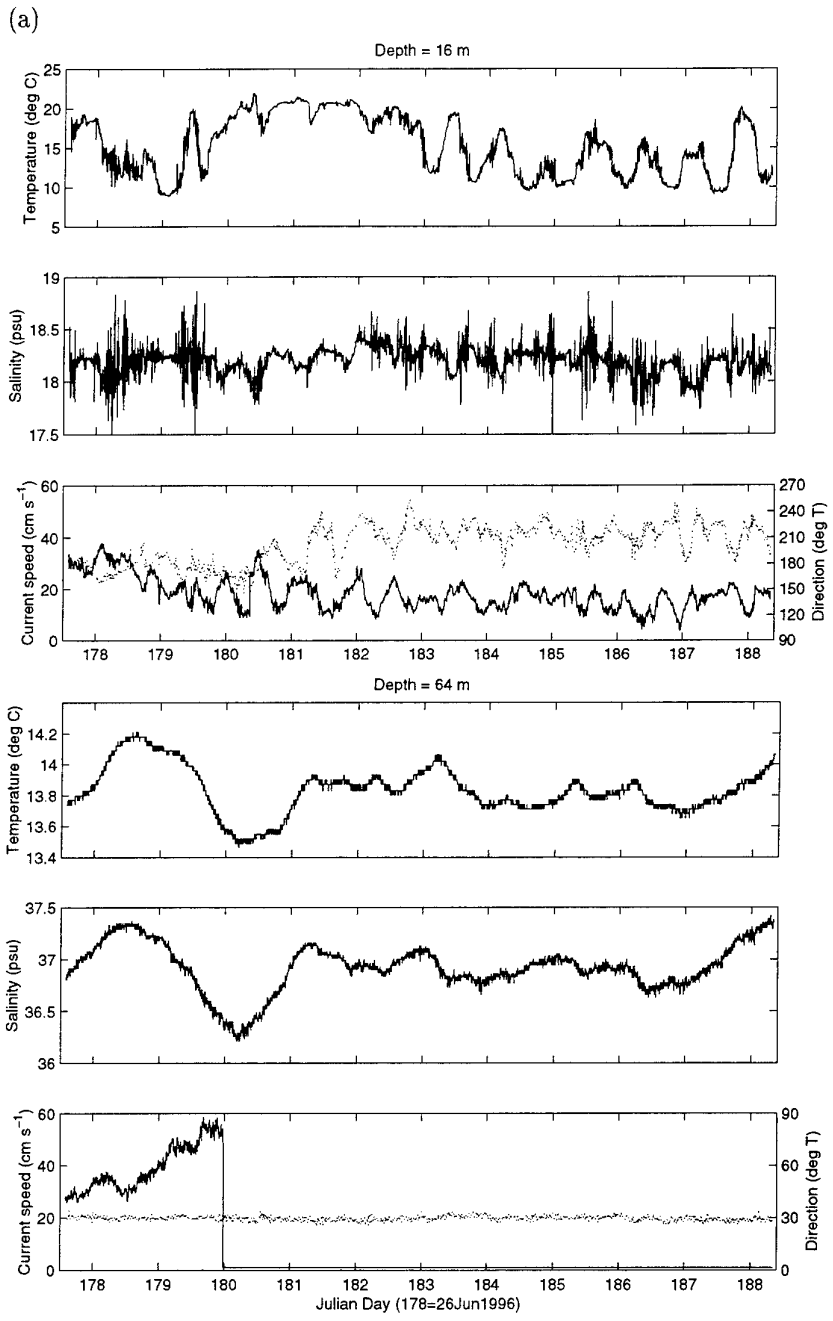

Figure 7 *Current meter data from (a) Mooring 1, South and (b) Mooring 2, North of the sill. Current direction is shown as a dotted curve.*

(b)

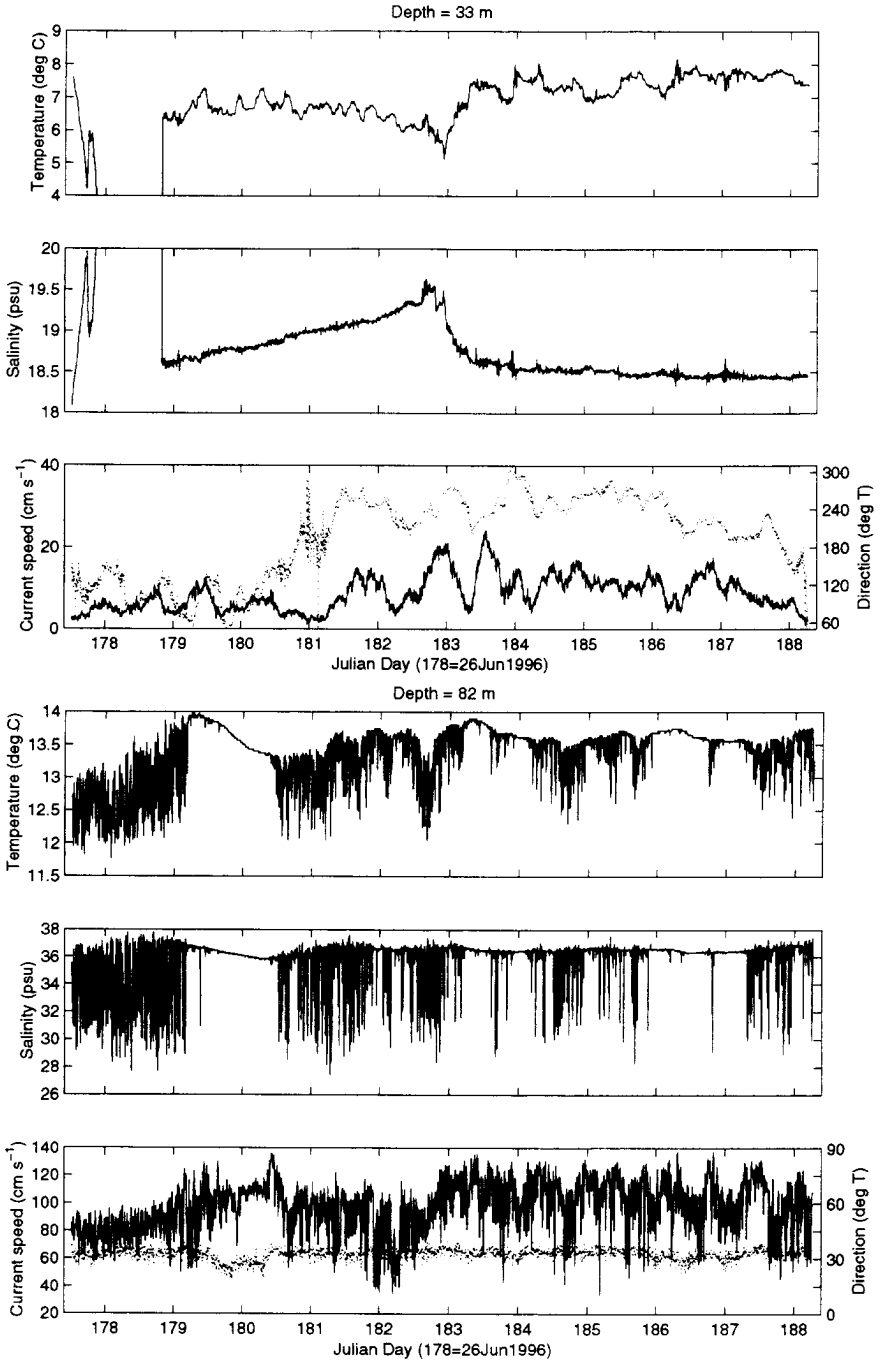

Figure 7 continued.

Mooring 1 Instruments	9556	12019
Instrument on	24JUN1996 16:19 UTC	24JUN1996 16:20 UTC
Start time	25JUN1996 13:59 UTC	25JUN1996 14:00 UTC
End time	6JUL1996 8:09 UTC	6JUL1996 8:10 UTC
Sampling interval	5 min	5 min
Depth	15.8 m	64.1 m
Mooring 2 Instruments	9555	9584
Instrument on	24JUN1996 16:19 UTC	24JUN1996 16:20 UTC
Start time	25JUN1996 12:14 UTC	25JUN1996 12:15 UTC
End time	6JUL1996 6:24 UTC	6JUL1996 6:25 UTC
Sampling interval	5 min	5 min
Depth	32.6 m	82 m

Table 3 *Current meter instrument parameters.*

rotor on this current meter was clogged by seaweed and hence failed on Julian day 180. The direction shows that the Mediterranean undercurrent follows the direction of the underwater canyon. When the current becomes maximal both the temperature and salinity approach minima and when the current is low the temperature and salinity approach maxima. This may be the result that when the undercurrent is strong, entrainment upstream (i.e. in the Strait of Istanbul) reduces both the temperature and salinity.

North of the sill (see Figure 7(b)) at 33 m depth the current meter was placed within the cold intermediate water of the Black Sea. At first the temperature sensor was not working, which affects the salinity calculation, but then after 1.5 days good measurements were obtained. The variability in temperature and salinity suggests the onset of an oceanographic front on Julian day 183 two days after which the current changed direction from an eastward flow to a westward flow.

The current meter data at 82 m depth shows strong fluctuations on all sensors. The variability on the temperature sensor and hence on the salinity are questionable since there are periods where no large fluctuations occur. The variability in the current speed, however, is associated with the turbulent nature of the Mediterranean flow plunging down the sill slope. Current speeds exceed 1 $m\ s^{-1}$ in this region. The flow follows the direction of the underwater canyon.

3.4 Thermistor chain

Thermistor chains were placed on each mooring so as to identify the interface variability between Black Sea and Mediterranean Sea water. Table 4 lists the relevant parameters describing the placement of the chain and the data collection times. To

Mooring 1 Instrument	1403
Instrument on	24JUN1996 17:19 UTC
Start time	25JUN1996 14:19 UTC
End time	6JUL1996 8:09 UTC
Sampling interval	10 min
Sensor depth	17.0 27.0 30.0 33.0 36.0 39.0 42.0 45.0 50.0 55.0 60.0 m
Mooring 2 Instrument	578
Instrument on	24JUN1996 19:19 UTC
Start time	25JUN1996 12:19 UTC
End time	6JUL1996 6:19 UTC
Sampling interval	10 min
Sensor depth	34.5 44.5 47.5 50.5 53.5 56.5 59.5 62.5 67.5 72.5 77.5 m

Table 4 *Thermistor chain instrument parameters.*

obtain confirmation of the thermistor chain and current meter placement and temperature values, CTD profiles were carried out before and after the deployment of each mooring. Figure 8(a) and (b) compares the temperature from the CTD profiles, thermistor chain and current meters for each mooring respectively.

The temperature profile at mooring 1 shows good agreement for all depths. For the profiles at mooring 2, the last three sensors on the thermistor chain record low temperature values. The shallow current meter temperature is shown only for placement and not for magnitude since the sensor did not work properly in the beginning (see Figure 7(b)). Also the deep current meter temperature may read low because of the large variability.

Images of the temperature variability from the current meters and thermistor chains are shown in Figure 9(a) and (b) from mooring 1 and 2 respectively. The colour scale is the same for both images and the depth spans 50 m. The temperature image for the mooring 2 location must be interpreted with caution since the lower three thermistor sensors read low. However, the interface depth and its variability can be seen.

¿From the 10 ^oC contour line of Figure 9 the interface depth is calculated and hence the layer thickness is determined as a function of time. The Froude number at the Mooring 1 location where $g' = 0.127\ m\ s^{-2}$, is typically $F^2 < 0.1$ indicating the flow is sub-critical. Since the lower current measurement was fouled by seaweed, the current from the scintillation technique (as will be shown) is used to evaluate the Froude number south of the sill.

The Froude number north of the sill at the Mooring 2 location gives values ranging from $F^2 = 0.1$ to 0.4 for $g' = 0.119\ m\ s^{-2}$ indicating that the flow is also subcritical. The supercritical flow regime according to the model results of Oğuz et al. (1990)

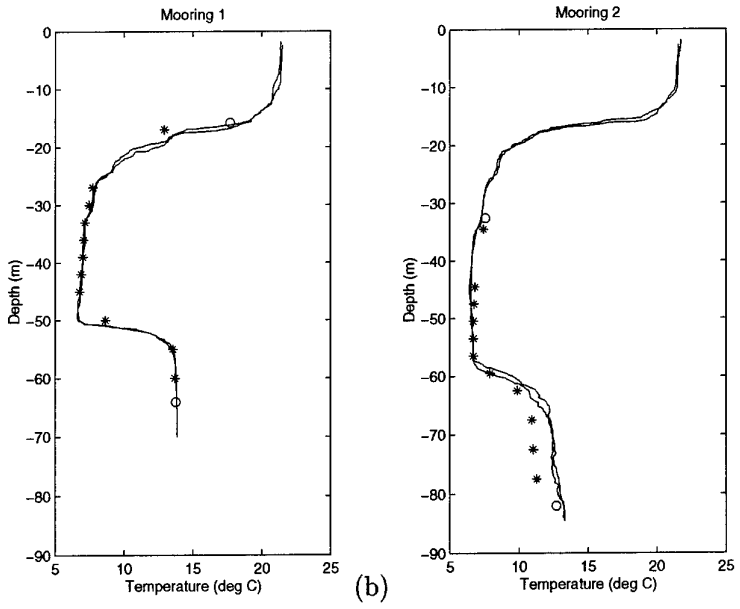

Figure 8 *Temperature profiles from the thermistor chain (*) and current meters (o) for comparison to CTD profiles taken before and after deployment (solid curve). (a) Mooring 1 and (b) Mooring 2.*

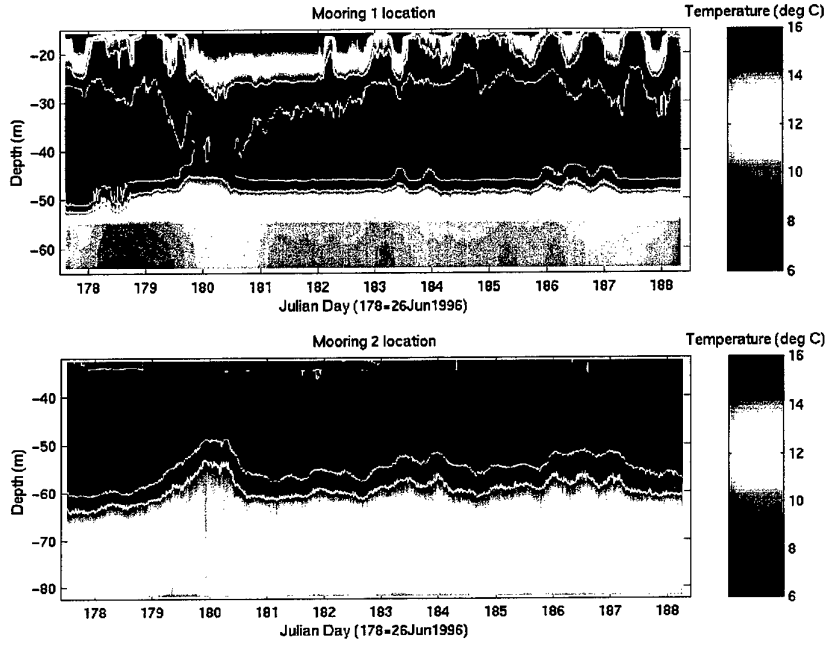

Figure 9 *Thermistor chain data with current meter temperatures from (a) Mooring 1 and (b) Mooring 2.*

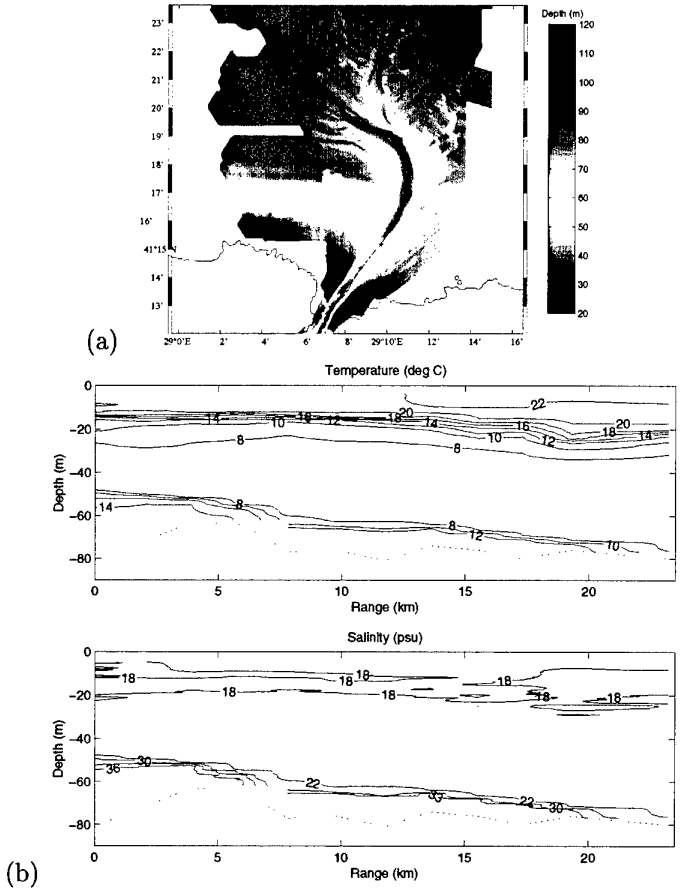

Figure 10 *(a) Bathymetry with CTD stations along the canyon superimposed. (b) Contours of temperature and salinity profiles. Bathymetry is shown as a dotted line.*

encompasses a region of 1 km north of the control point (hence 2 km north of the sill crest). Our measurements are taken approximately 2.5 km from the sill crest and therefore are just outside the region where supercritical flow is expected. It is expected that the flow remains subcritical along the continental shelf.

3.5 CTD profiles and time series

CTD profiles taken along the canyon over 23 km distance (see Figure 10(a)) are shown as contours of temperature and salinity in Figure 10(b). The decrease in salinity through the canyon occurs on average at a rate of 0.28 $psu\ km^{-1}$.

TCG *Çubuklu* of the DNHO obtained CTD time series at an anchored station (see Figure 2). These time series consisted of profiles approximately every half hour and once an hour the CTD was deployed at 55 m depth for a 10 min time series of oceanographic properties. This temporal variability in temperature and salinity structure is used to determine the amount of mixing in the dense lower layer, as well as the interface of the two layer system.

Figure 11 shows colour images of the temperature and salinity variability with contours superimposed. During this 24 h period the thermocline depth at 20 m varied by a few meters. This variability is caused by a deepening of the thermocline which can be seen more clearly in the thermistor chain temperature images of Figure 9. During this time period the Black Sea current at approximately 20 m (as seen by the ADCP and current meter results) undergoes periodic oscillations in the southeasterly direction implying advection of warm surface waters which results in a change in the thermocline depth. The Mediterranean inflow during the CTD measurement period was most intense and hence very little variation in the interface structure.

The temperature-salinity (T-S) relation for all the profiles is shown in Figure 12 together with contours of sigma-t and sound speed evaluated at 0 dbar pressure; pressure effects on sound speed over 60m depth is approximately 1 $m\ s^{-1}$ and therefore has been ignored for these contours. The sound speed difference between Black Sea and Mediterranean Sea water is 40 $m\ s^{-1}$ and the density difference is 14 $kg\ m^{-3}$. Salinity effects on sound speed in this environment is important since the soundspeed contours are diagonal instead of horizontal.

Three distinct water masses are seen from the T-S diagram: the surface Black Sea water ($T = 22^oC$, $S = 18psu$), Black Sea cold intermediate water ($T = 7.5^oC$, $S = 18.2psu$) and the Mediterranean bottom water ($T = 14^oC$, $S = 36psu$). Between these water masses lies strong mixing regions.

Figure 13 and 14 show 10 min temperature and salinity time series respectively taken over a 24 h period at a depth of 55 m which at this location is 5 m below the interface. All the data is documented in this report so that the temporal variability in temperature and salinity can be seen. During the time of the measurement, the Mediterranean current was strong, having a speed of 0.6 $m\ s^{-1}$ as measured by the current meter south of the CTD anchor location. The sampling rate of 5 Hz limits the smallest scale sensitivity to 24 cm during a maximum flow of 0.6 $m\ s^{-1}$. Thus it is the larger scales that are measured.

¿From the time series measurement one can see variability in both the temperature and salinity as a result of the periodic motion of the surface waves. The surface waves cause the CTD to oscillate up and down as the ship rocks back and forth. Figure 15 shows the depth of the CTD on Julian day 180.31 over an elapsed time of 7 min together with the power spectral density. The spectral peak at frequency 0.16

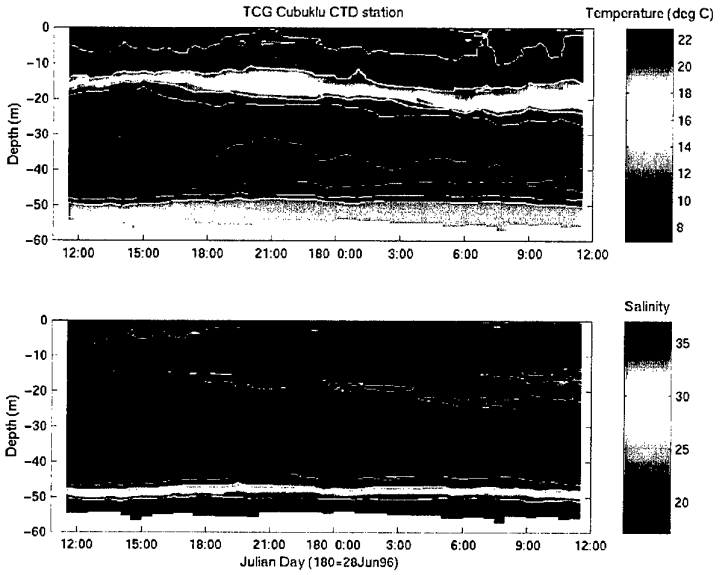

Figure 11 *Temperature and salinity profile time series taken by TCG Çubuklu at their moored station. Contours for temperature are [8 10 12 14 16 18 20 22] °C and for salinity [18 20 25 30 35] psu.*

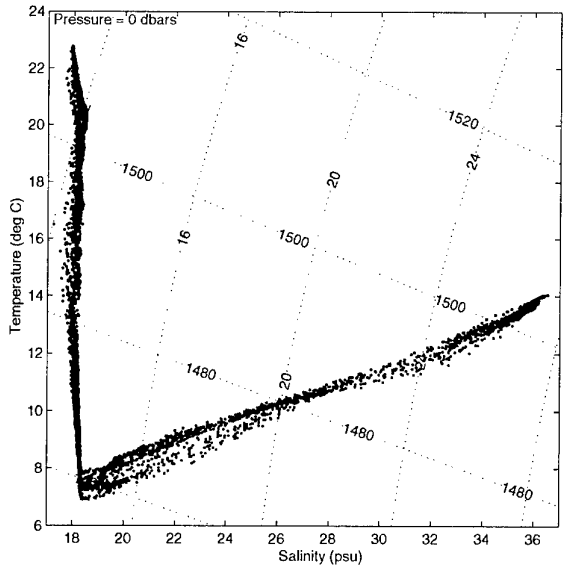

Figure 12 *Temperature versus salinity for the profiles shown in Figure 11. Contours of sigma-t and sound speed evaluated with no pressure effects are also shown.*

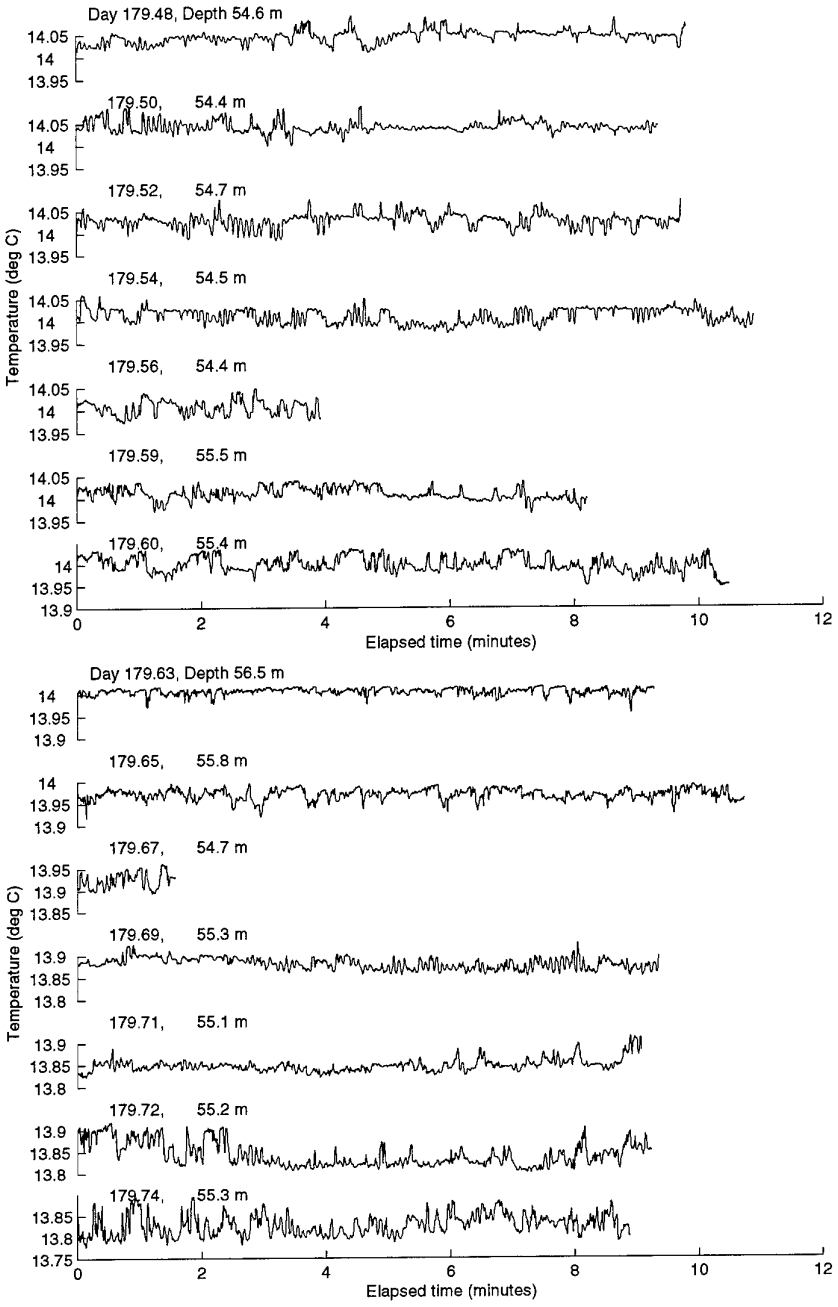

Figure 13 *Temperature time series taken by TCG Çubuklu at the moored station.*

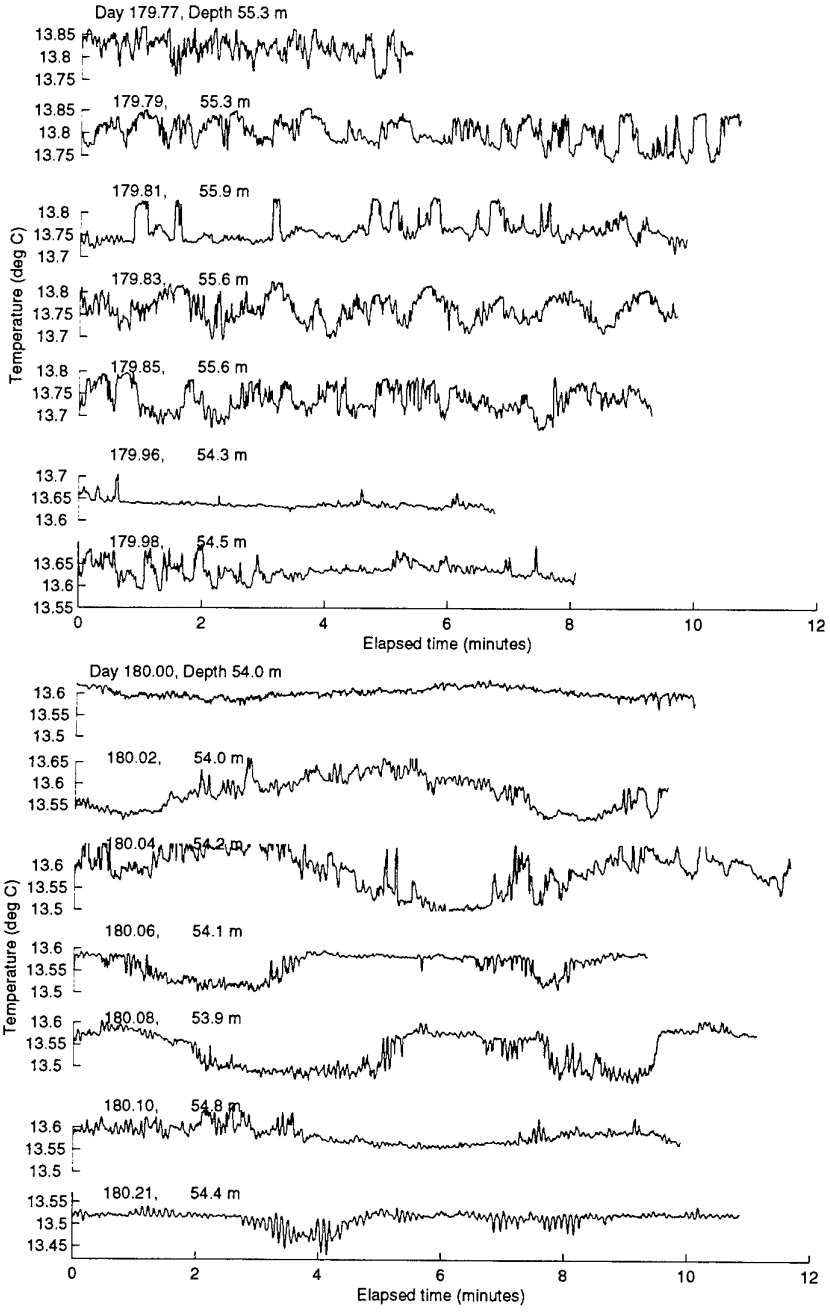

Figure 13 continued.

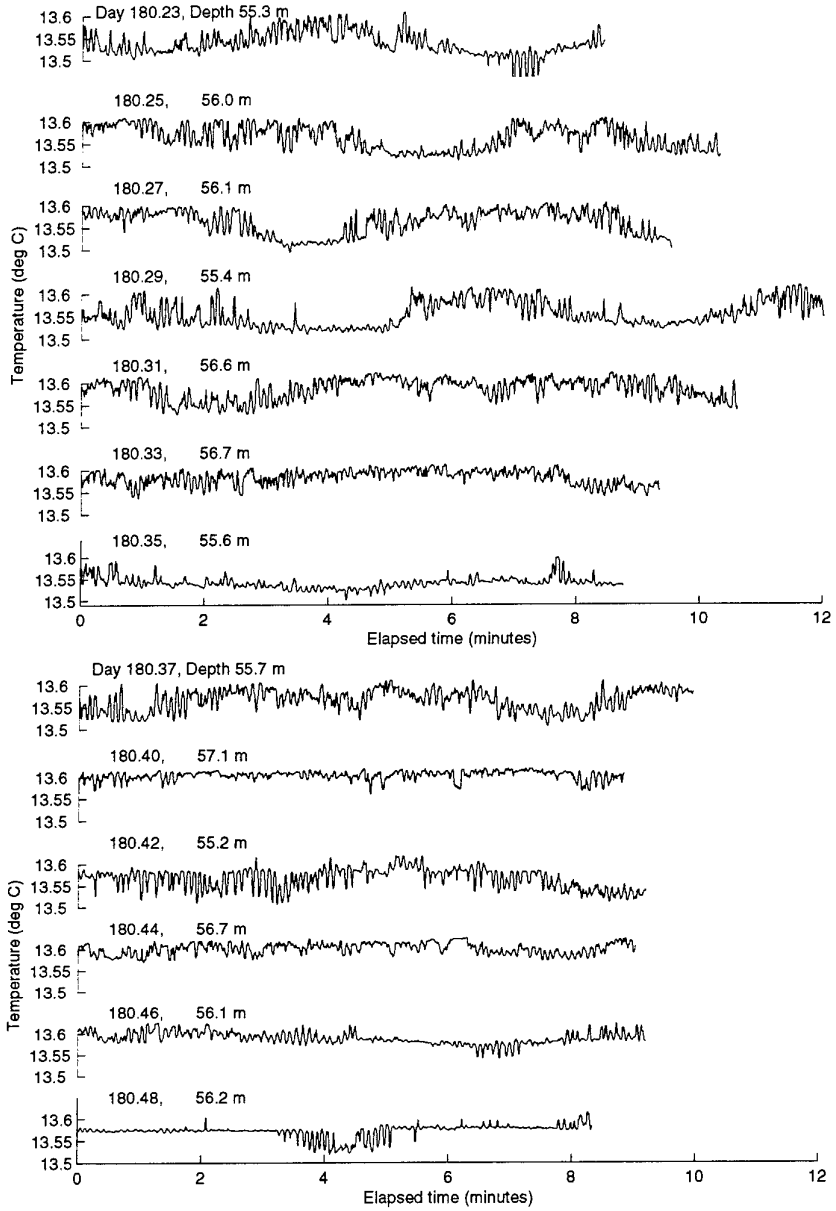

Figure 13 continued.

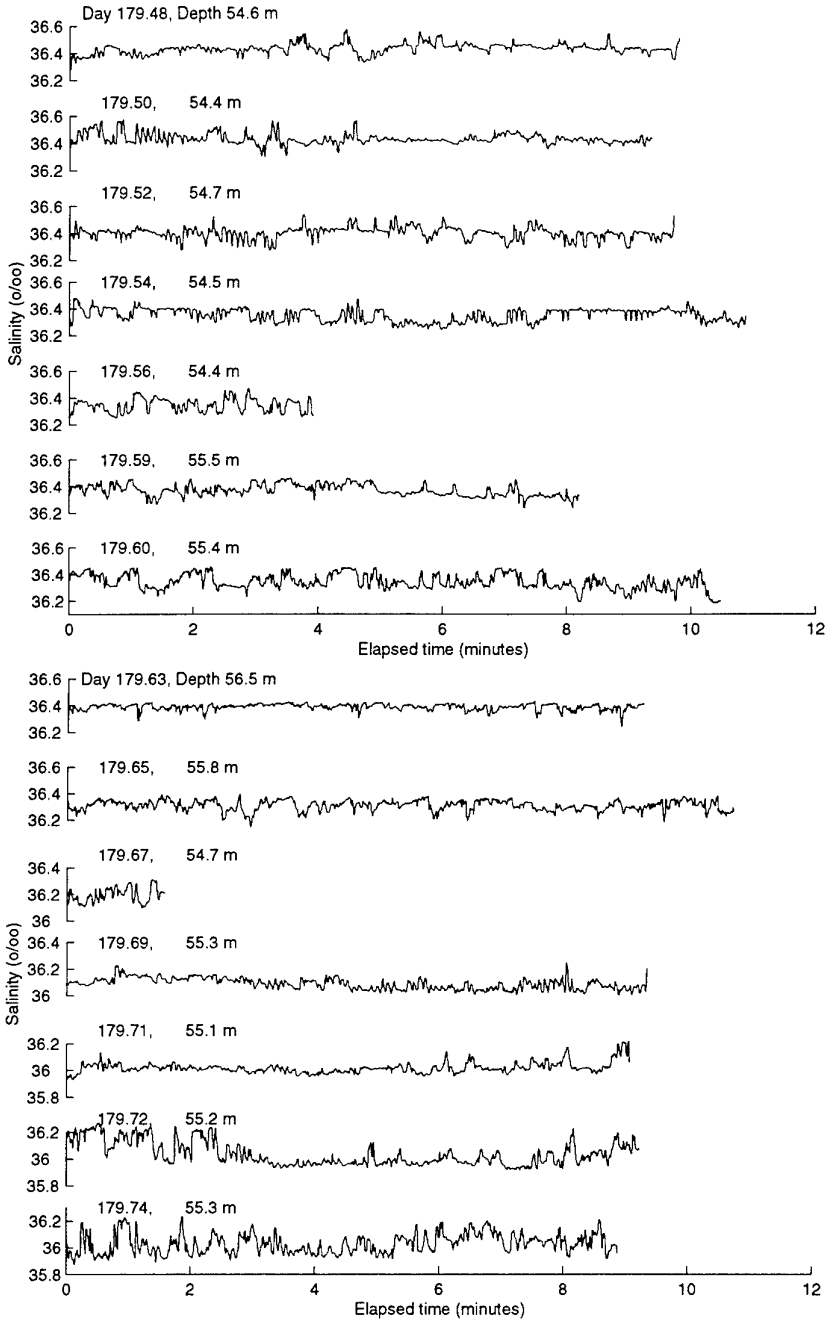

Figure 14 *Salinity time series taken by TCG Çubuklu at their moored station.*

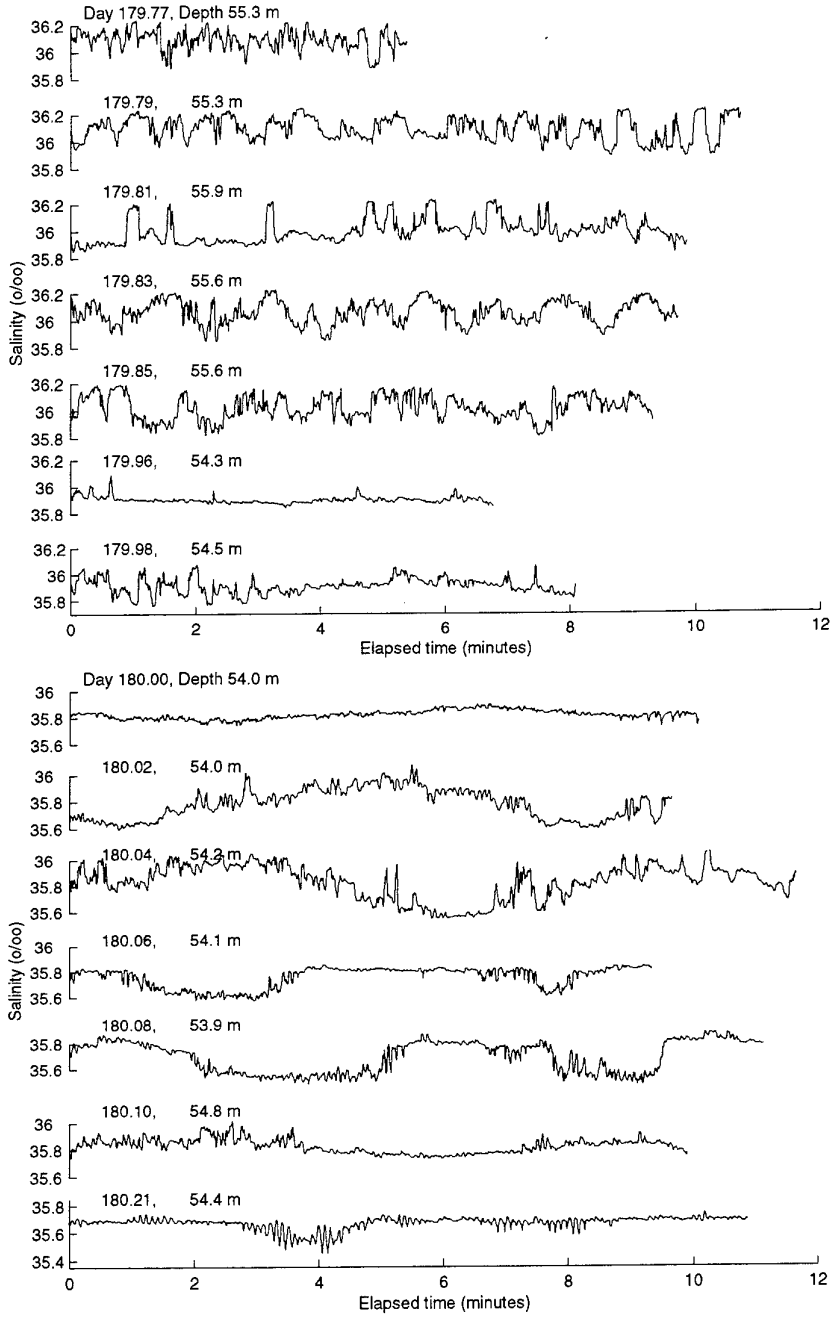

Figure 14 continued.

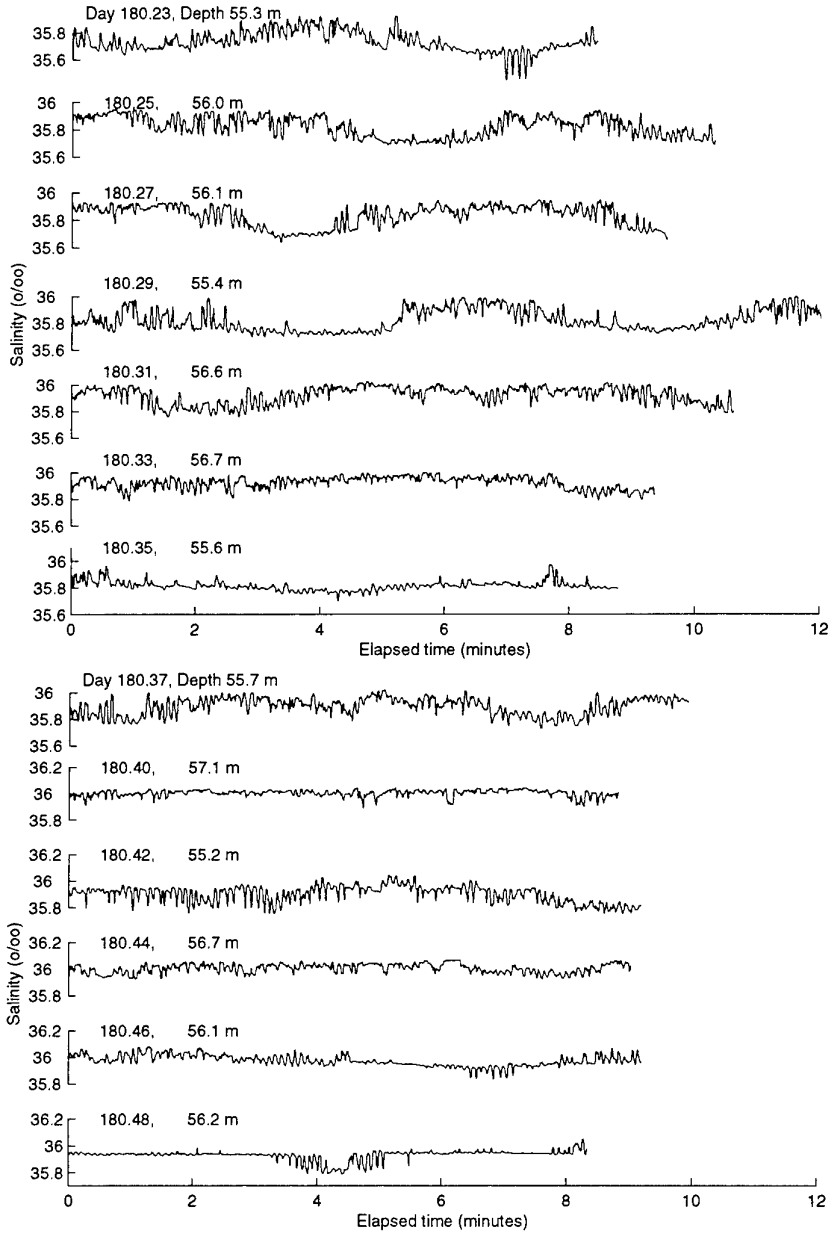

Figure 14 continued.

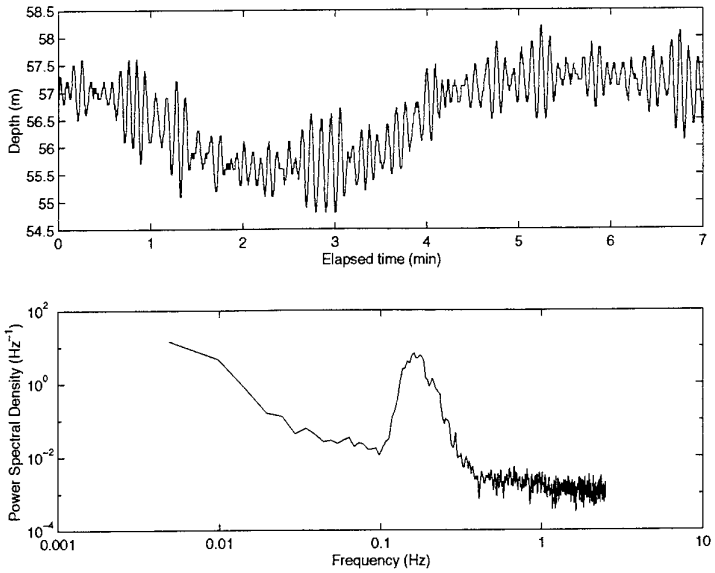

Figure 15 *CTD depth as a function of elapsed time together with the power spectral density.*

Hz corresponds to sea surface wave motion of 6 s wave period and 1.5 m peak-to-peak wave height. Changes in depth of approximately 1 m cause temperature and salinity variations of order $1°C$ and 1 psu respectively.

3.6 Acoustic scintillation

A high frequency (307.2 kHz) acoustic scintillation system with two transmitters and two receivers (on loan from the Institute of Ocean Sciences, Sidney, B.C. Canada) was deployed in the same location as the 1995 sea trial described by Di Iorio and Yüce (1999). Table 5 summarizes the experimental parameters used during this deployment - the primary difference is the transmission rate.

Sample acoustic scintillation data (approximately 2 min) are shown in Figure 16 during a time of strong and weaker flow. Much variability in the amplitude exists during strong flow because of the turbulent nature of the flow. The travel time difference between the two parallel paths shows a periodic nature as a result of mooring oscillations. When the current weakens the acoustic amplitude variability diminishes as a result of reduced turbulent levels. The travel time difference oscillations are also reduced (see Figure 16).

The statistics for the normalized log-amplitude $\chi = \ln(A/ < A >)$ (where A is

Parameter	quantity
Start time	26-JUN-96 7:00 UTC
End time	01-JUL-96 18:00 UTC
Transmission rate	10 Hz
Frequency	307.2 kHz
Pulse width	0.1 ms
Pulse delay	20 ms
Digitization rate	153600 Hz (1 sample/2 cycles)
Path length	369 m
Propagation direction	311 deg T
Transducer separation	0.2 m
Depth (T/R)	62.5/65.5 m

Table 5 *Acoustic scintillation instrument parameters.*

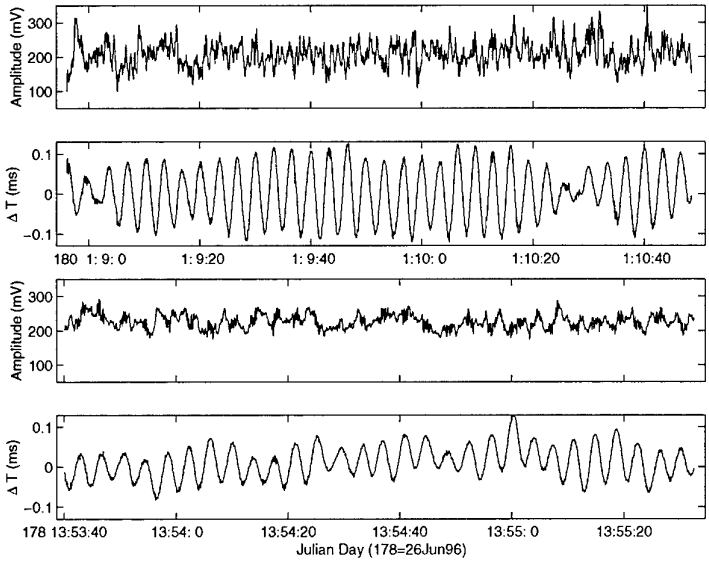

Figure 16 *Sample acoustic scintillation data when the Mediterranean undercurrent was strong ($U = 0.6\ m\ s^{-1}$ on Julian day 180 1:10 UTC) and weak ($U = 0.3\ m\ s^{-1}$ on Julian day 178 13:54 UTC).*

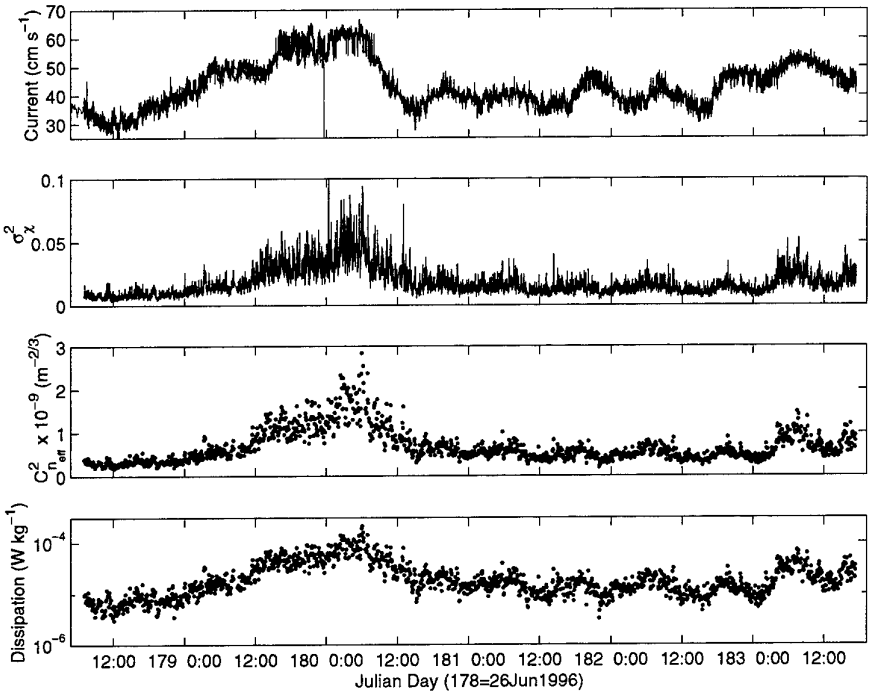

Figure 17 *Current speed from the acoustic scintillation technique together with current meter data where available, the log-amplitude variance, effective refractive index structure parameter and the turbulent kinetic energy dissipation rate throughout the measurement period.*

the acoustic amplitude and <> denotes a time average), allow measurement of oceanographic parameters as discussed by Di Iorio and Yüce (1999). The current speed is calculated by measuring the time delay of the log-amplitude cross covariance function between the two parallel acoustic paths. The results are shown in Figure 17 together with available current meter measurements at depth 64 m for comparison. Over the 5 day measurement period much variability exists in the flow. The log-amplitude variance σ^2_χ is also shown in Figure 17 and the variability follows the current speed. During maximum flow the log-amplitude variance is maximal.

The level of the effective refractive index fluctuations defined by,

$$C^2_{n_{eff}} = C^2_{n_s} + \frac{11}{6} C^2_{n_v} \tag{2}$$

(Di Iorio and Farmer, 1998) is expressed in terms of the refractive index fluctuations arising from temperature and salinity variability (scalars) and those arising from the current variability (vectors). The log-amplitude variance allows measurement of

$C^2_{n_\epsilon ff}$ through the equation,

$$\sigma^2_\chi = 0.124 C^2_{n_{\epsilon ff}} k^{7/6} L^{11/6}, \tag{3}$$

where k is the acoustic wavenumber and L is the acoustic path length. Note that the acoustic amplitude variability cannot distinguish between fine scale variability from scalars and that from current. The dominant scale size which contributes to the log-amplitude variance as discussed by Tatarskii (1971) is the Fresnel radius $\sqrt{\lambda L} = 1.2\ m$. The measurement of $C^2_{n_{\epsilon ff}}$ is also shown in Figure 17.

Independent measurements of the temperature/salinity structure cannot be compared to the scintillation measurement. This is because the CTD time series were taken at 55 m depth close to the interface and also because the time series shows oscillations indicative of sea surface wave motion. Previous measurements in this area, however, showed that turbulent velocity dominated the acoustic scattering. Also, since the log-amplitude variance and hence the level of the effective refractive index variability vary according to the increasing and decreasing current, it can be assumed that temperature/salinity variations have negligible effect on acoustic forward scatter.

Since velocity fluctuations dominate the acoustic scattering, some interesting oceanographic parameters describing the turbulent boundary layer can be calculated. For example the turbulent kinetic energy dissipation rate is determined via (Di Iorio and Farmer, 1994),

$$\epsilon^{2/3} = \frac{C^2_{n_v} c_o^2}{1.97}, \tag{4}$$

where c_o is the mean sound speed at the depth of the acoustic path. Acoustic measurements of ϵ in Figure 17 range from 3×10^{-6} to $1 \times 10^{-4}\ W\ kg^{-1}$. Assuming that the measurements are made in a constant stress layer the bottom drag coefficient is determined from (Monin and Ozmidov, 1985),

$$\frac{C_D^{3/2} U^3}{\kappa z} = \epsilon, \tag{5}$$

where $\kappa = 0.4$ is von Karman's constant and $z = 10\ m$ is the distance from the bottom boundary. Measurements range from 5×10^{-3} to 15×10^{-3}. These values are consistent with the measurements made during the West Black 1995 sea trial (Di Iorio and Yüce, 1999).

3.7 Echo soundings

To compliment the data from moored instrumentation and profiling instruments, towed echo soundings were obtained along the canyon in the Black Sea exit region. The acoustic characteristics and operating parameters for the Biosonics echo

Parameter	quantity
Source level	215.3 dB re 1 μPa @ 1 m
Beam width	3.8^o
Pulse width	0.2 ms
Transmission interval	0.4 and sometimes 0.3 s
Time variable gain	$20 \log r$

Table 6 *Echo sounding instrument parameters.*

sounder are shown in Table 6. The narrow beamwidth together with the small pulse length and fast transmission rate allows high resolution measurements of the two layer structure. Sound is scattered by small fish, zooplankton, and temperature microstructure.

Figure 18 shows a 30 km transect of high resolution imaging of the two layer flow together with XBT profiles of temperature superimposed. The interface and sea bottom are identified by the dark red/black colours which correspond to strong acoustic back scatter levels. Acoustic energy is scattered from temperature microstructure and from biological matter which tends to accumulate at the interface (Farmer and Denton, 1985). Much spatial variability is observed in the flow as a result of mixing between Mediterranean bottom water and Black Sea cold intermediate water. This flow visualization helps interpret the profiles of temperature.

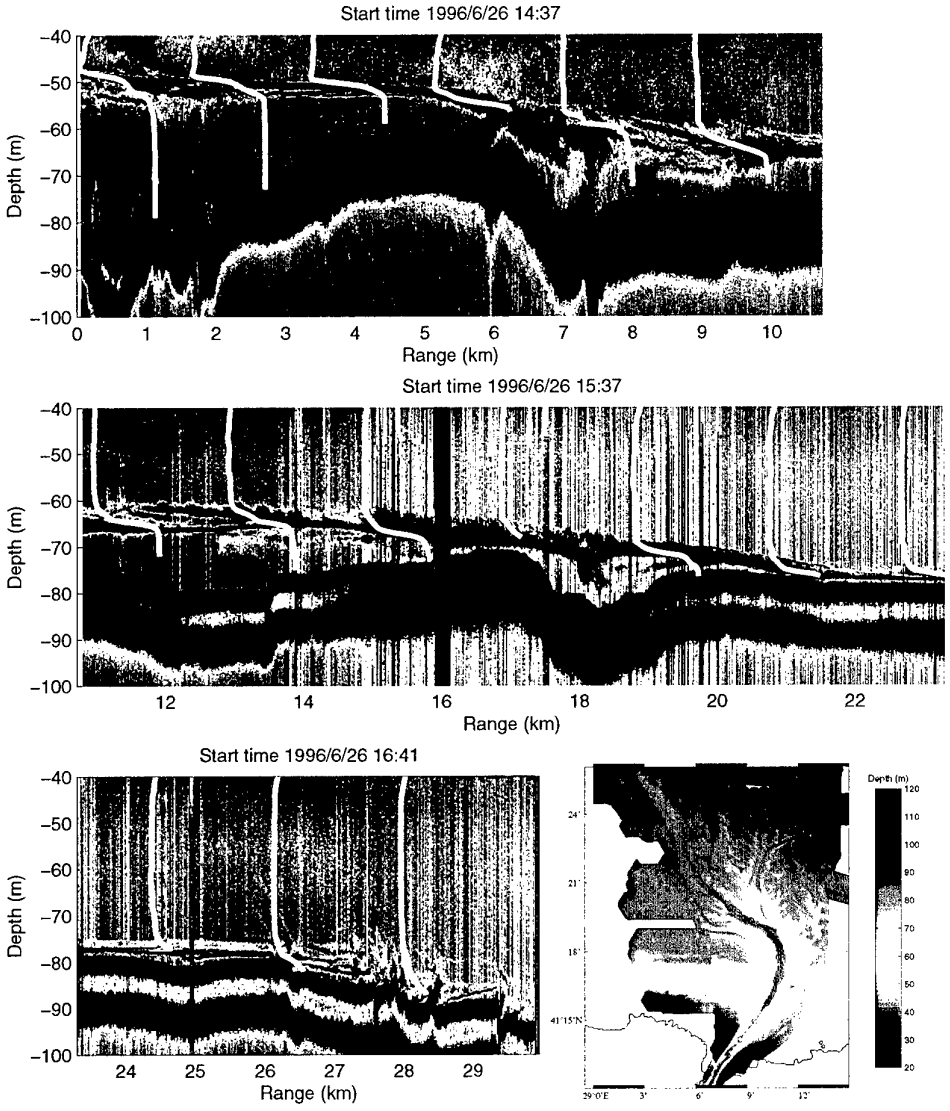

Figure 18 *Transect along the canyon with high resolution echo soundings together with temperature profiles from expendable sensors. Colour levels correspond to the acoustic back scatter levels with strong levels being red/black and weak levels blue.*

4

Continental Shelf Region

One basic provision in studying Black Sea and Mediterranean Sea water exchange is knowing where the dense Mediterranean water finds its way along the shelf toward the slope and the resulting mixing that takes place with the cold intermediate water of the Black Sea. On the shelf the Mediterranean flow follows a 'delta' like structure and the salinity dilution is expected to occur quite rapid compared to mixing within the Strait.

In studying this area the multi-beam SWATH echo sounder was used to obtain detailed bottom bathymetry adding to the Black Sea 1995 measurements. CTD, XCTD, XBT profiles and occasional time series of current from a Neils Brown acoustic current meter (NBIS) and CTD were obtained on the continental shelf so as to locate the Mediterranean effluent and measure its characteristics (see Figure 19). In addition, a high resolution, high frequency (120 kHz) echo sounder was used along the ship track to locate the Mediterranean water and thus obtain two dimensional imaging of the two layer flow structure. The 100 m contour line approximates the start of the continental slope.

4.1 CTD, XCTD and XBT profiles

The profiles of temperature (from CTD, XCTD and XBT) and salinity (from CTD and XCTD) taken on the shelf as indicated by Figure 19 are shown in Figure 20. The presence of Mediterranean water is indicated by the increase in temperature to $12^{o}C$ and the increase in salinity to 34 psu at the bottom of the profiles. Whenever possible the CTD profiles were taken close to the bottom but it is possible that some of them did not reach the Mediterranean water since its thickness is just a few meters on the bottom. The Mediterranean water was primarily located in the region of the underwater canyon and its presence was also observed close to the 100 m contour east of the canyon as a result of spreading. Deep Black Sea water has a salinity of 22.3 psu beyond 1000 m and thus values greater than this represents the presence of the Mediterranean effluent.

Measurements within the canyon show that the Mediterranean effluent decreases in salinity as a result of mixing with the Black Sea intermediate water at a rate of 0.1 $psu\ km^{-1}$. This rate is almost a factor of three different from the rate observed

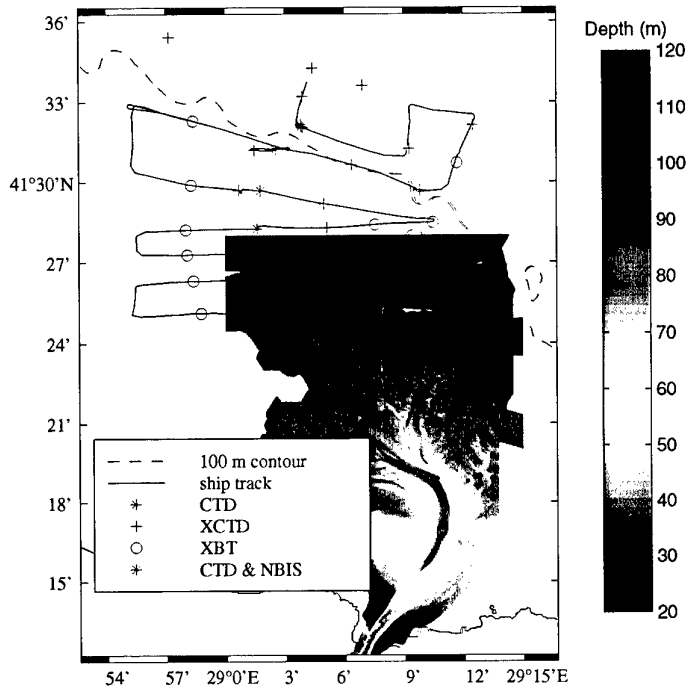

Figure 19 *Map showing locations of CTD, XCTD, XBT and NBIS measurements. Echo sounding images are obtained along the ship tracks shown.*

in the canyon exit region. One reason for the reduced spatial mixing rate could be that the flow does not reach supercritical conditions (as will be shown); supercritical flow results in increased turbulent mixing.

4.2 Current and CTD time series

Occasional time series of the current, temperature and salinity of the Mediterranean bottom water on the continental shelf was attempted. The CTD instrument cage was equipped with a Neils Brown acoustic current meter (NBIS) so that the whole unit could be placed on the sea floor for a short time series of water properties. The acoustic current meter instrument was set to obtain 1 min averaged samples and the results were output on paper and are shown in Table 7. The instrument was on the sea bottom when the vertical velocity was close to zero.

Salinity time series were obtained at a 25 Hz sample rate and two point averaged data are shown in Figure 21. Some of the time series correspond to the current time

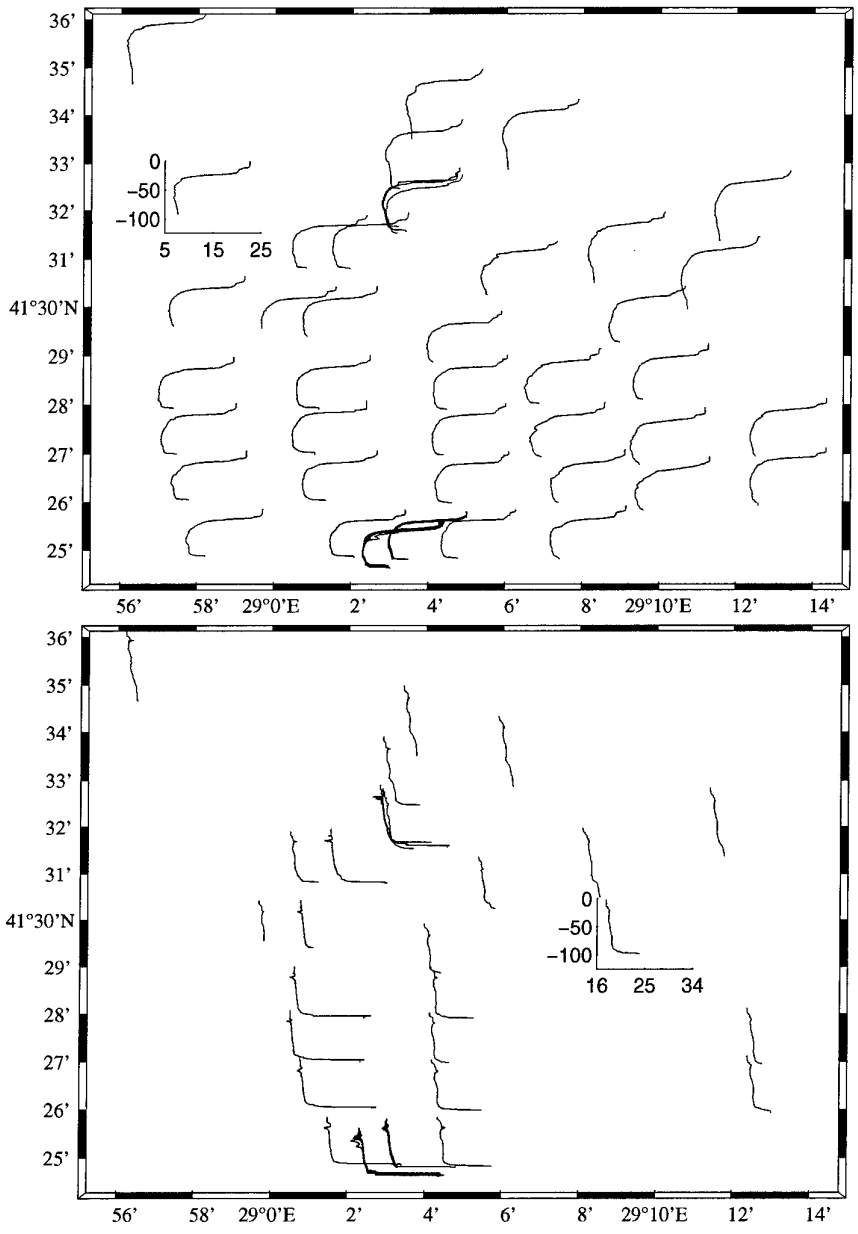

Figure 20 *Profiles of temperature (top) and salinity (bottom) plotted at their geographic location. Profiles are taken from Julian day 178.708 (26/6/1996 1700) to 179.708 (27/6/1996 1700).*

Julian Time (UTC)	Z (cm/s)	E-W (cm/s)	N-S (cm/s)
170 19:17	-30.38	7.14	-0.56
19:18	0.63	4.76	12.6
19:19	-0.77	6.72	11.62
19:20	0.63	1.54	9.38
19:21	0.5	1.42	9.67
19:22	0.57	1.99	10.1
19:23	0.28	1.85	9.39
19:24	0.14	1.71	10.24
19:25	13.01	-2.13	6.68
178 18:12	-44.59	-4.85	1.25
18:13	-0.28	-14.96	1.8
18:14	0.83	-14.54	9.42
18:15	0.9	-13.43	5.54
18:16	-10.8	-11.36	1.94
179 04:51	-12.35	13.52	-0.28
04:52	-2.97	1.52	-3.45
04:53	-1.52	2.35	-3.31
04:54	-2.07	2.62	-3.45
04:55	-2.14	2.62	-3.31
04:56	-2.21	2.35	-3.04
04:57	-2.35	2.76	-3.17
04:58	-2.28	2.48	-3.17
04:59	3.59	35.73	12.83
05:00	22.9	14.07	7.86
179 09:31	-12.73	36.18	12.73
09:32	0	18.31	5.15
09:33	-0.72	10.73	0.29
09:34	2.15	15.59	3.58
09:35	-2.29	20.31	17.88
181 08:22	-29.52	-0.14	6.76
08:23	-0.56	0.28	5.49
08:24	-0.21	1.41	5.35
08:25	-0.28	1.55	0.42
08:26	-0.56	1.41	1.97
08:27	0.35	0.28	0.56
08:28	-0.21	2.96	1.13
08:29	0.14	2.82	2.4
08:30	0.77	0.85	0.56
08:31	-0.92	0.99	-2.41
08:32	0.28	3.27	5.97
08:33	13.93	10.52	13.93

Table 7 *Neils Brown Acoustic Current meter results.*

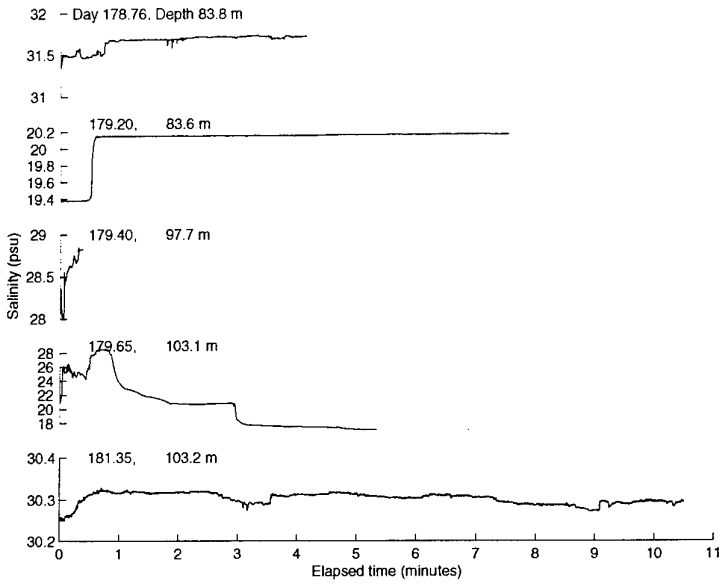

Figure 21 *Time series of bottom salinity taken on the continental shelf.*

Julian Time (UTC)	$< Z >$ (cm/s)	Mag (cm/s)	Dir (^oT)	S (psu)	σ_t
178 18:14	0.48	15.4	291	31.5	23.9
181 08:28	-0.07	2.5	44	30.3	23.0

Table 8 *Summary table for current and CTD measurements.*

series shown in Table 7 and the length depended on weather conditions since the instrument cage was cabled to NRV *Alliance*. On Julian day 179.2 the instrument was not placed within Mediterranean water; on Julian day 179.4 the unit had to be recovered quickly so that the instrument did not drag along the bottom; on Julian day 179.65 it initially was placed well within Mediterranean water but then was possibly dragged to where Mediterranean water was absent.

Of the five measurements of current and CTD time series, only two measurements were obtained simultaneously with a length of time necessary for reliability. They are summarized in Table 8 and the locations are shown in Figure 19. The current for the southern site is toward the northwest having magnitude 15.4 $cm\ s^{-1}$ and salinity 31.5 psu, whereas at the northern site the flow is reduced to 2.5 $cm\ s^{-1}$ toward the northeast with salinity 30.3 psu. These directions correspond to the direction of the canyon and slope shown in Figure 19. Calculation of the Froude number for these two locations give $F^2 < 0.1$ confirming that flow along the shelf is subcritical.

4.3 Ship mounted ADCP measurements

Table 9 are the set up parameters for the hull mounted 75 kHz ADCP system for surveying the continental shelf. The current vectors for the survey in Figure 19 are shown in Figure 22 averaged over the specified depth interval. The current vectors show a cyclonic circulation pattern over the 100 m depth contour. This flow pattern exists over the whole measurement depth from 20 to 70 m.

4.4 Echo sounding images

Echo sounding images are obtained along the ship track shown in Figure 19 in order to provide some interpretation for the profiles of temperature and salinity shown in Figure 20. The results for each transect are shown in Figure 23 where the first image (at the top) corresponds to the southernmost transect. The first five images correspond to the 5 southernmost transects and the last three images correspond to the last northernmost horizontal transect which is broken up into three overlapping sections.

From these images the spreading extent of the Mediterranean bottom water is seen to the east and west of the major canyon located at the 8 to 10 km range. These images also show that the continental shelf bathymetry is a complex pattern of ridges and troughs. The major canyons which transport the Mediterranean water are identified out to the start of the continental slope. From the dimensions of the canyon (for the first horizontal transect) together with the flow velocity made within this canyon, the transport of Mediterranean water is estimated to be $1.2 \times 10^3\ m^3\ s^{-1}$.

Parameter	quantity
Bin length	4 m
Transmission interval	1.5 s
Sample interval	5 min

Table 9 *75 kHz ADCP instrument parameters.*

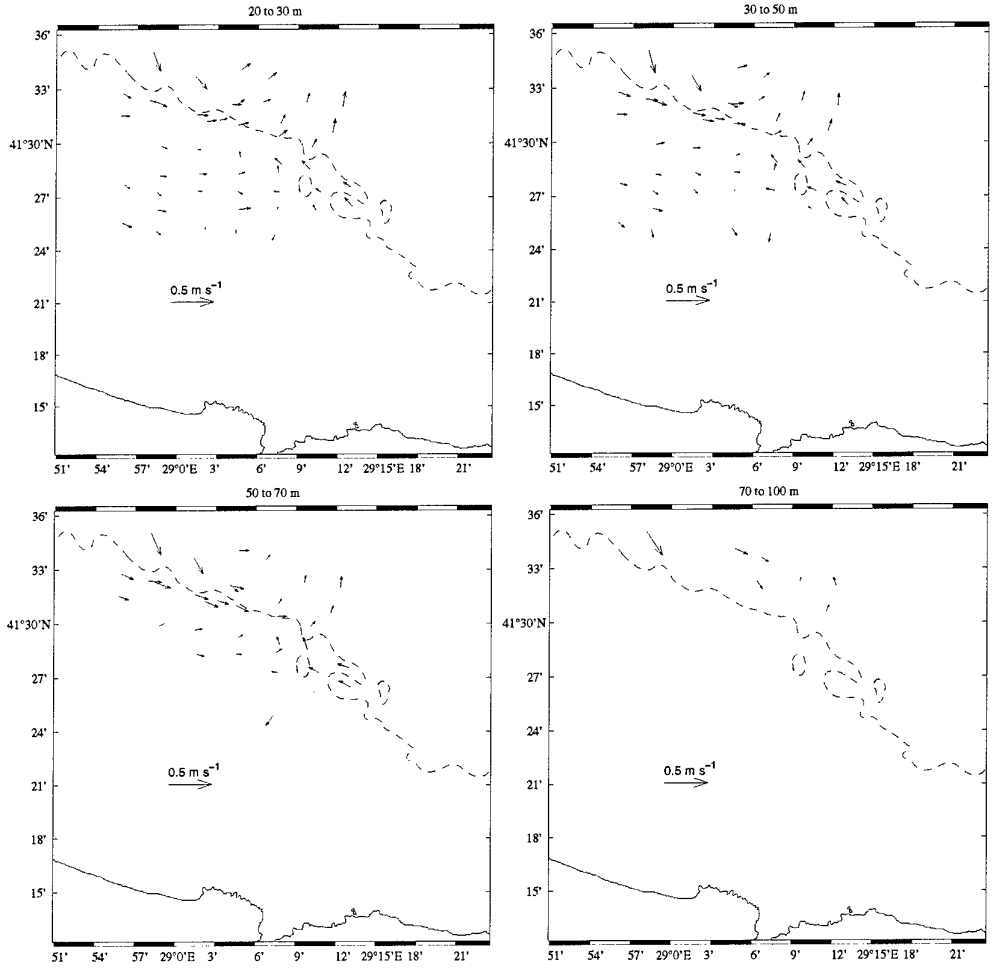

Figure 22 *Current vectors averaged over the specified depth interval.*

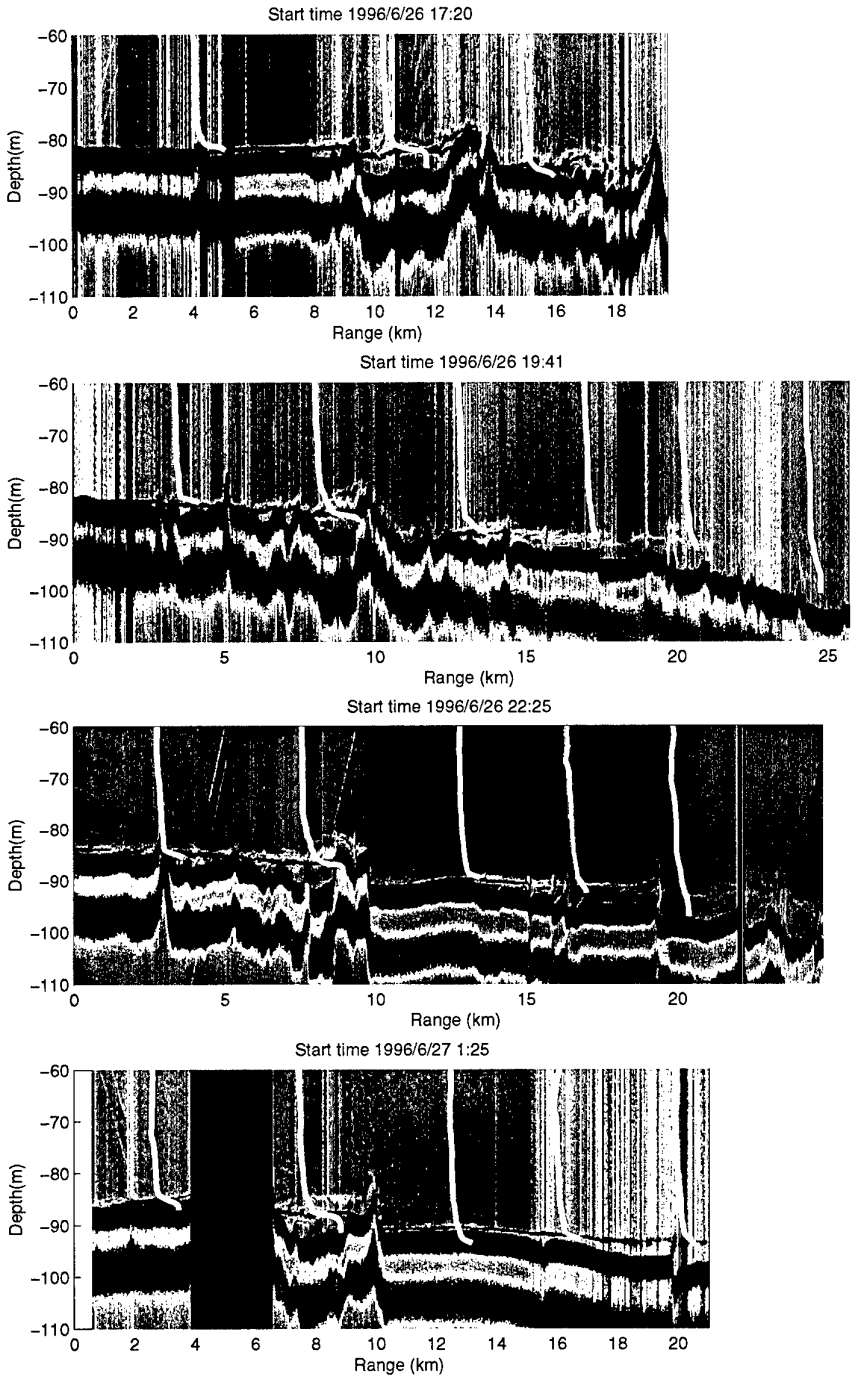

Figure 23 *Transect across the shelf with high resolution echo sounder imaging together with temperature profiles from profiling sensors. Colour represents the acoustic backscatter intensity where red/black is strong backscatter and blue is weak backscatter.*

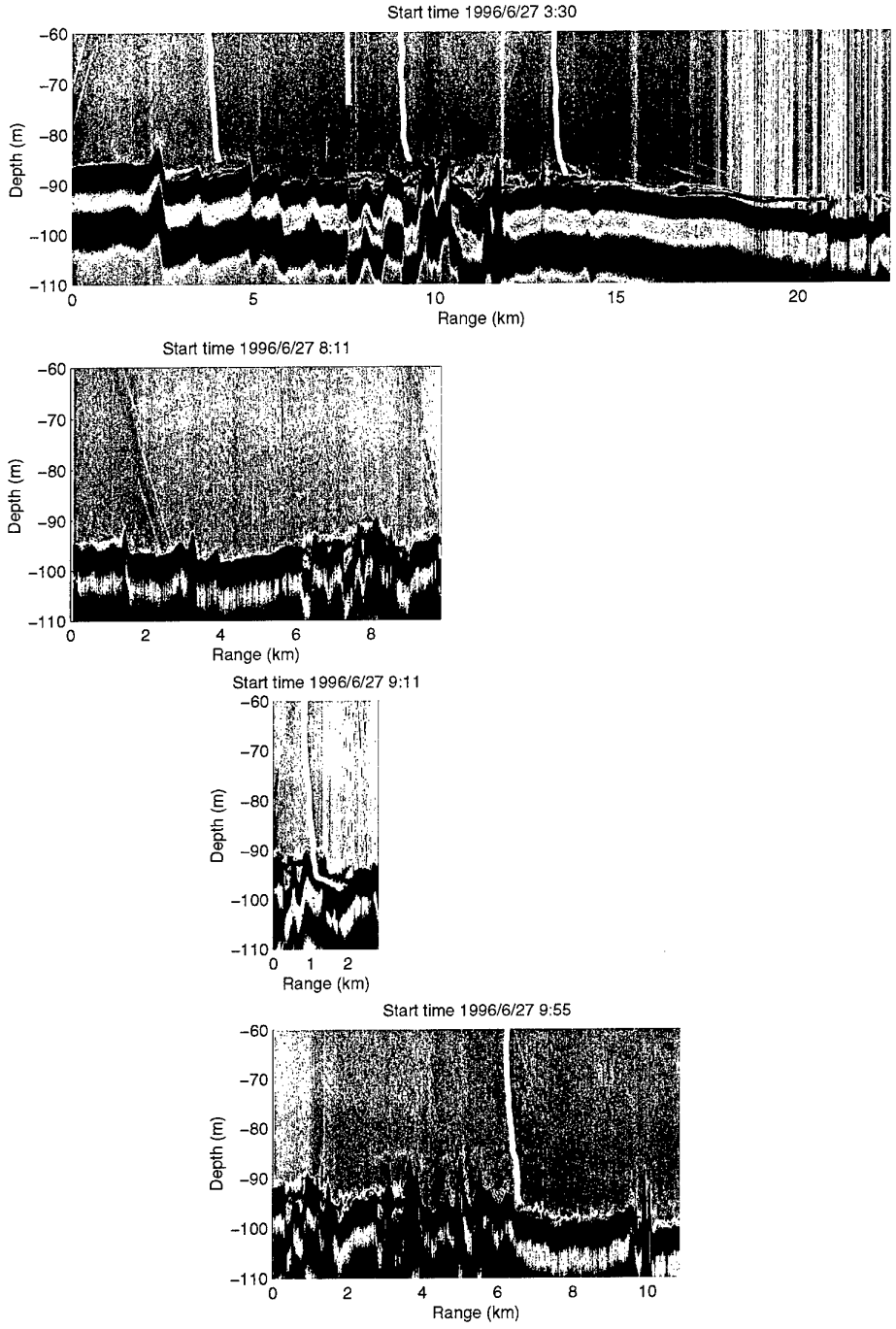

Figure 23 continued.

5

Continental Slope / Deep Sea Region

Beyond the shelf the diluted Mediterranean sea water sinks down the continental slope to a depth appropriate to its density and is then incorporated in the eastward general circulation of the Black Sea. It is expected to be found as occasional intrusions differing in temperature and salinity from the surrounding water. With this in mind a large scale survey was carried out with measurements from CTD, XBT and XCTD profiles, and the 75 kHz ADCP system on board NRV *Alliance*. This large scale survey is complimented by NOAA satellite images of sea surface temperatures. Figure 24 shows the ship track for the large scale survey of the continental slope / deep sea region, with 100, 500 and 1000 m depth contours and the location of all profiles.

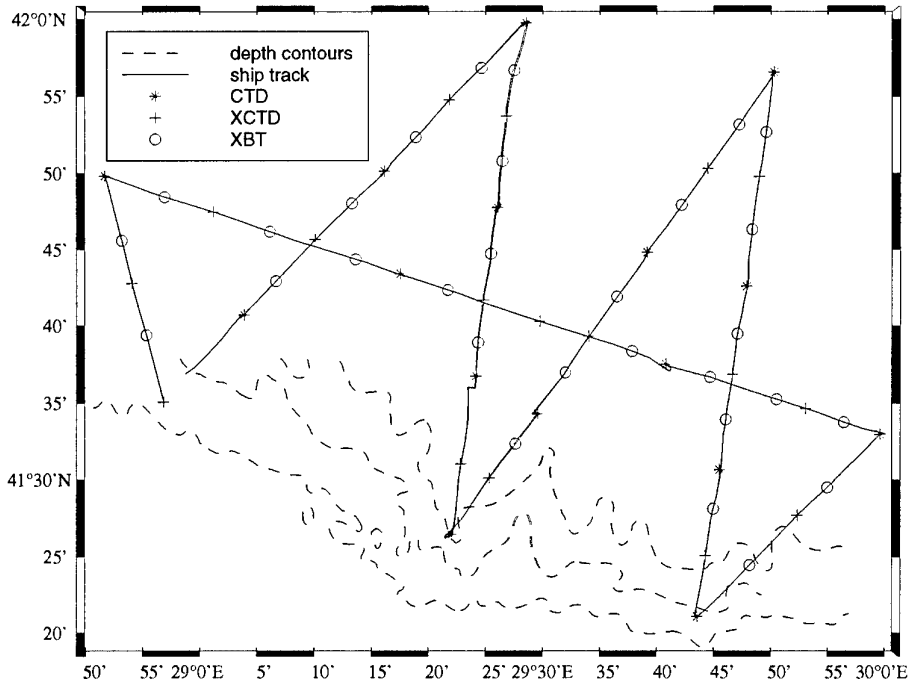

Figure 24 *Map showing locations of CTD, XCTD and XBT. Depth contours are for 100, 500 and 1000m. Profiles are taken from 27/6/1996 1700 to 29/6/96 0500.*

5.1 CTD, XCTD and XBT profiles

Profiles of temperature and salinity at their geographic locations are shown in Figure 25. Analysis of the temperature along the horizontal track shows little spatial variability in the temperature profile. The vertical tracks (from north to south) however show cold intermediate water (temperatures between 7 and 8 degrees C) down to 150 m depth on the southern side of the tracks which is toward the continental slope and at 100 m depth toward the northern deep sea part (see Figure 26). The salinity follows the same pattern where the 21 psu contour line deepens toward the continental slope. This characteristic is consistent with all the vertical tracks.

5.2 Ship mounted ADCP measurements

The 75 kHz shipborne ADCP was also used in this large scale survey and the results are shown in Figure 27 together with the continental shelf results. Two dominant features stand out. First, there is a general eastward circulation which is a permanent feature of the Black Sea (Oğuz and Rozman, 1991). Second, there is a wave-like modulation along the horizontal track which is persistent over the depth range of 20 to 150 m. The wavelength of this feature is approximately 70 km. This wave feature may be the result of the "β-effect" (the variation of the Coriolis parameter with latitude) and an eastward current might oscillate in this way if perturbed (Pond and Pickard, 1983). If a parcel of water is perturbed northward the Coriolis force will produce a restoring force causing flow to circulate clockwise. If the parcel of water then moves southward then a similar restoring force will occur in the opposite direction giving anticlockwise circulation. This motion is typical of Rossby waves.

Calculation of the Rossby radius of deformation $\lambda = \sqrt{g'h}/f \approx 63km$ where g' is the reduced gravity based on measurements of the density difference ($\Delta\rho/\rho = 2 \times 10^{-3}$) in the region, $h = 2000m$ is the depth and $f = 1 \times 10^{-4}$ is the Coriolis parameter. This estimation agrees well with observations.

5.3 Sea surface temperatures

The sea surface temperatures during times at which there was little or no cloud cover throughout the measurement period are shown in Figure 28. Land is denoted in white with a black outline. The oceanographic survey of the shelf and deep sea region covered the period June 26 to June 29 during which time no stable features could be seen in the infrared images of sea surface temperature.

The most striking feature in these images is the output of Black Sea water into the Sea of Marmara which shows up as a cold plume compared to the warm surrounding

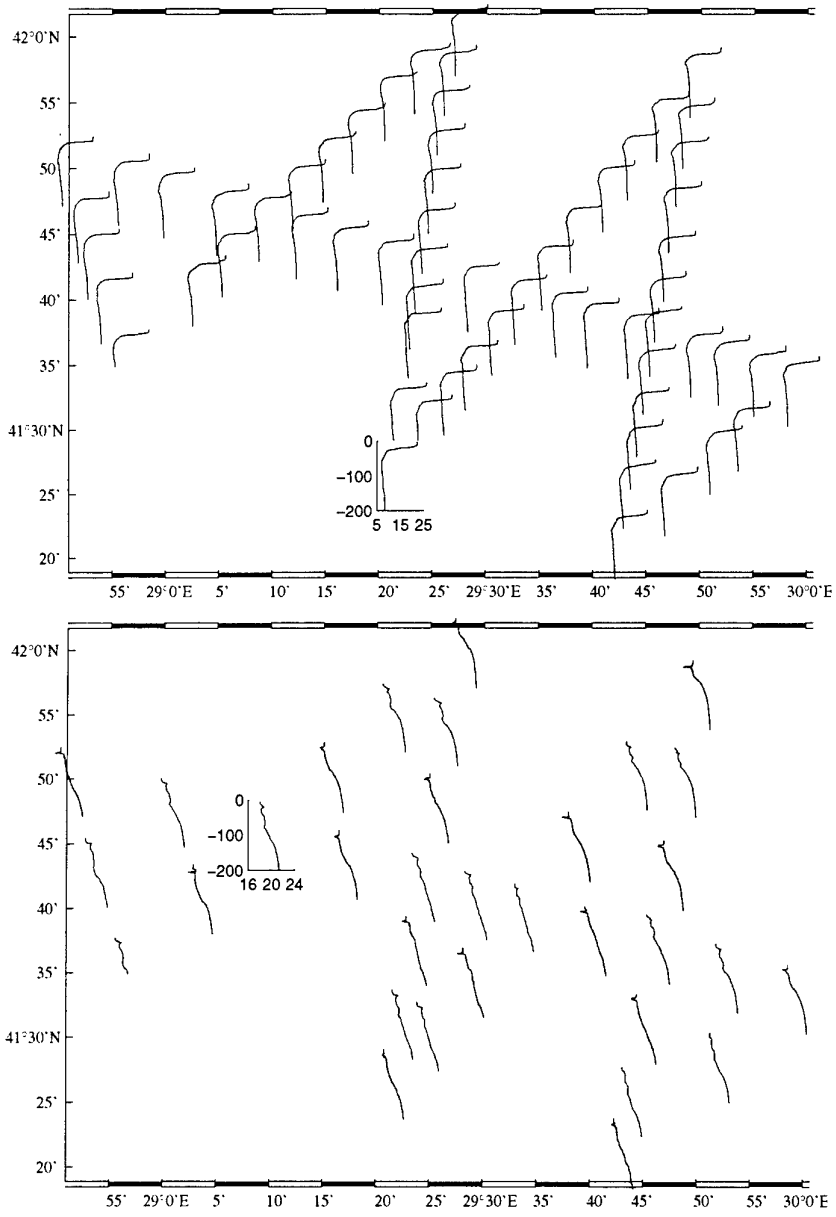

Figure 25 *Temperature and salinity profiles shown at their geographic location. Profiles are taken from Julian day 179.708 (27/6/1996 1700) to 181.208 (29/6/1996 0500).*

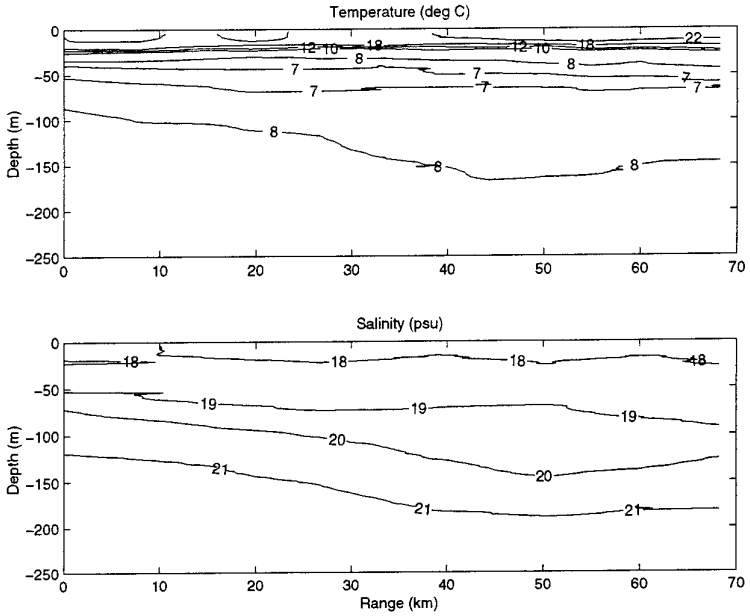

Figure 26 *Temperature and salinity contours taken along a vertical track from the northeast to the southwest direction.*

water. The Black Sea outflow veers to the right and forms an anticyclonic eddy which is most pronounced during the July measurement periods. For example on 02July96 16:25 UTC and 03July96 00:59 UTC the dark blue regions of the sea surface temperatures in the Marmara Sea show the advection of an anticyclonic eddy southwards.

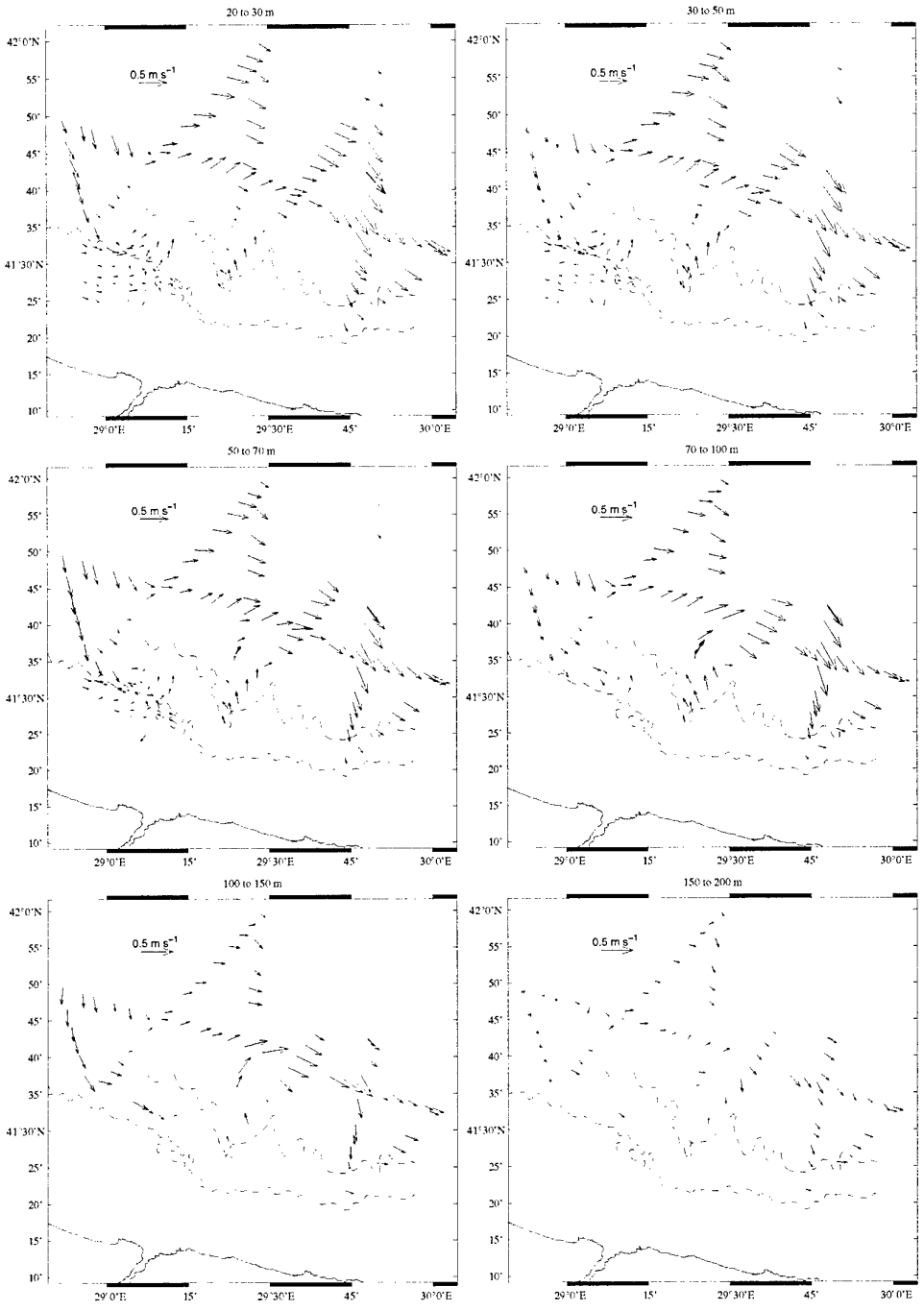

Figure 27 *Current vectors averaged over a depth interval.*

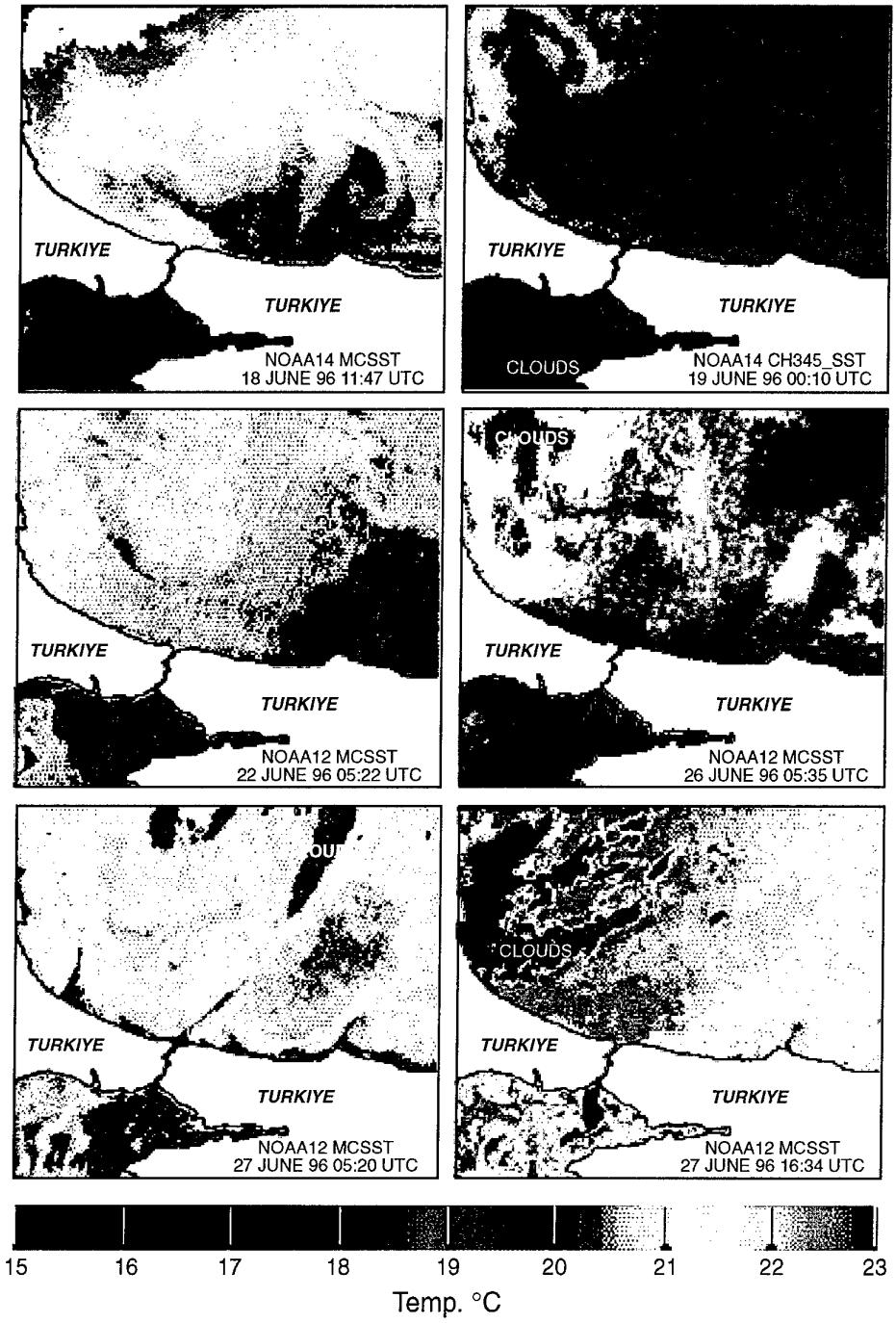

Figure 28 *NOAA Satellite images of sea surface temperatures.*

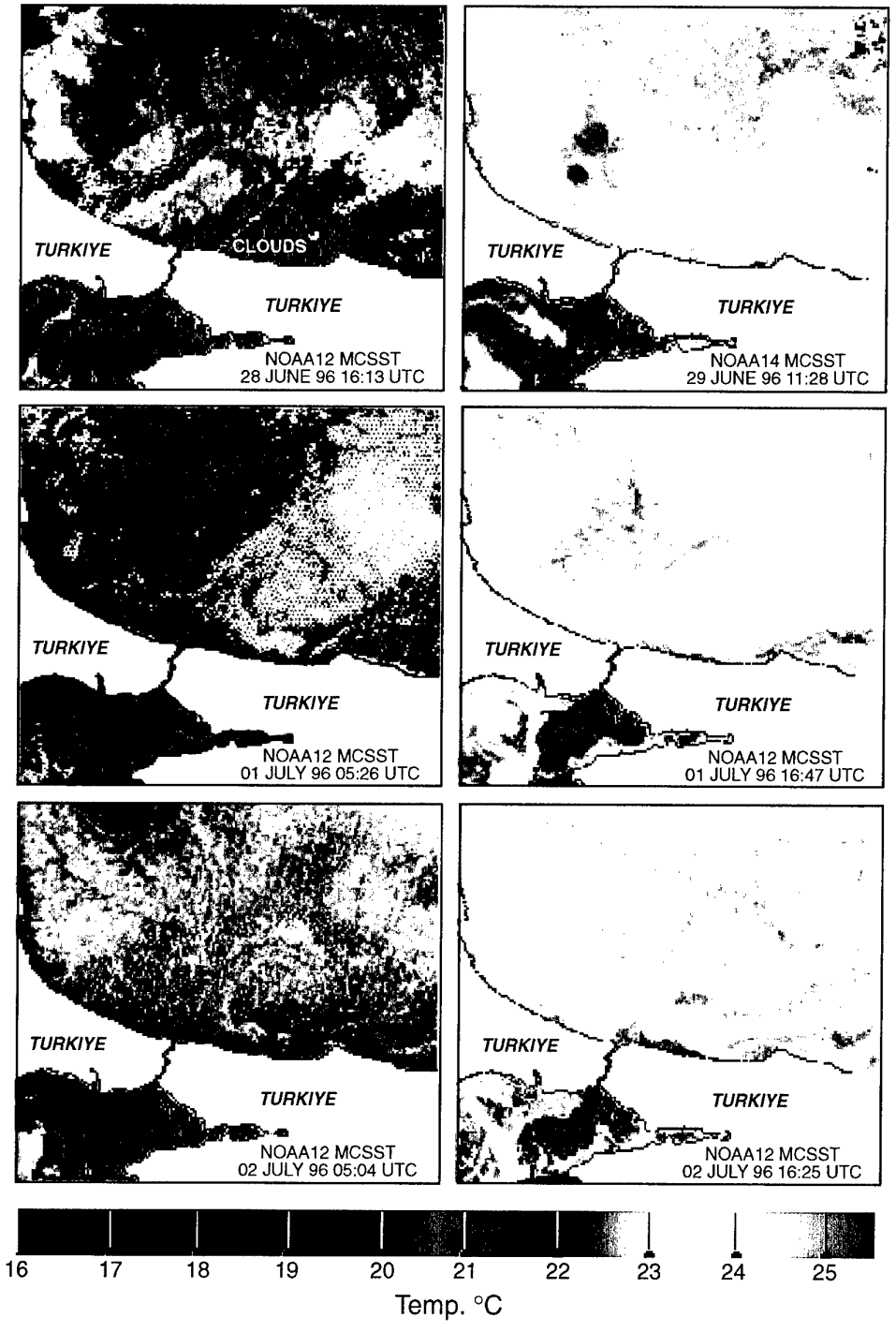

Figure 28 continued.

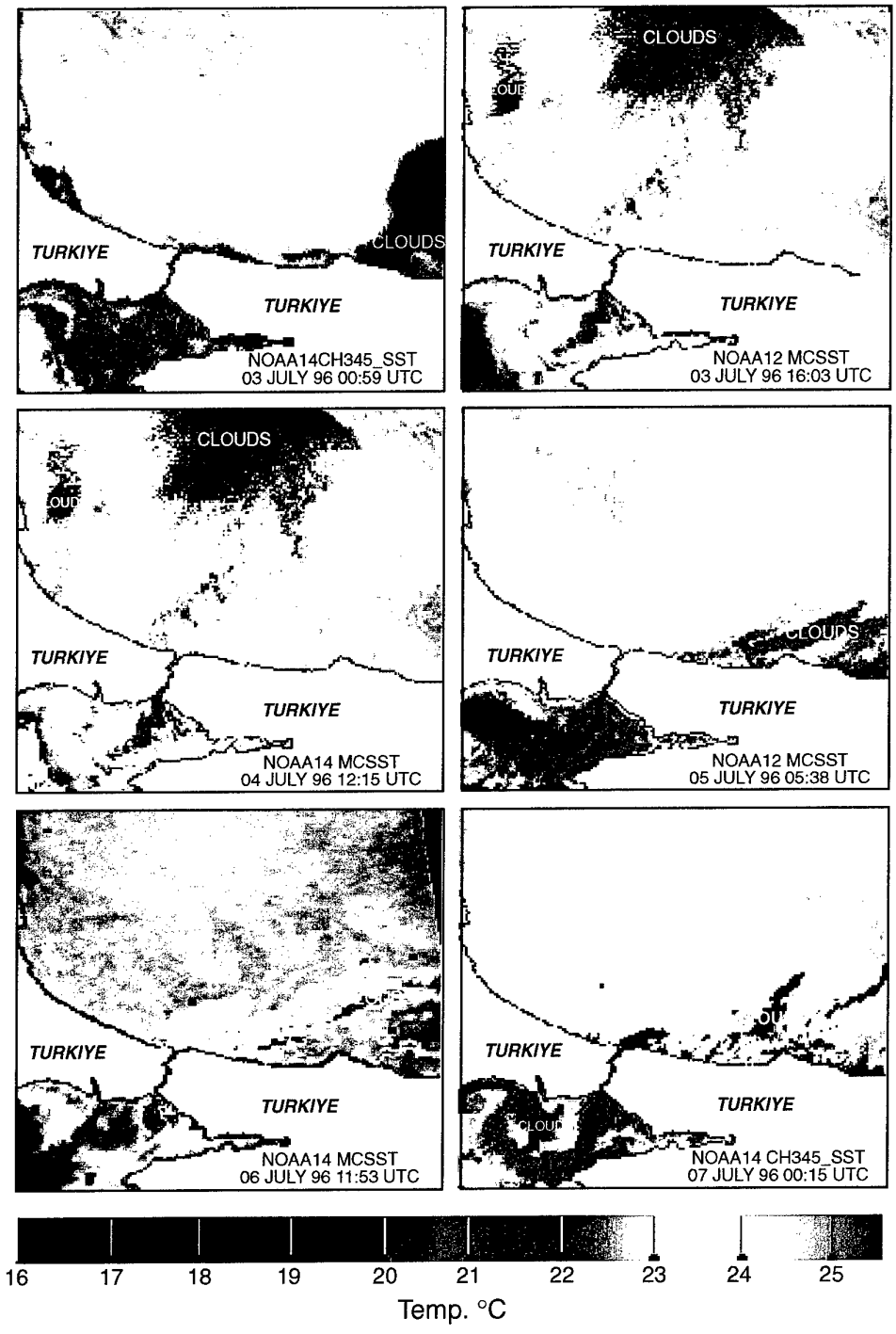

Figure 28 continued.

6
Conclusion

This report describes the oceanographic measurement program of the West Black Sea during the period June 15 to July 5, 1996. An extensive survey of the Black Sea exit region, continental shelf and deep sea region was carried out which leads to a better understanding of Mediterranean Sea water inflow.

Mediterranean water inflow during this measurement program was continuous. The strength of the flow followed the changing sea level difference between Anadolukavagi and Fenerbahce. Analysis of the flow in terms of hydraulic theory showed that the flow was sub-critical at our three mooring locations: south of the sill, on the sill and north of the sill. In order to observe the critical and super critical regimes of the flow precise mooring locations are required. Measurement of the turbulent kinetic energy dissipation rate showed strong levels of current velocity variations as a result of bottom and interfacial friction.

Extensive surveying with CTD along the canyon and continental shelf showed that the salinity along the canyon decreases at a rate of 0.3 psu/km and on the shelf at a rate of 0.1 psu/km. Measurement of the Mediterranean water on the continental shelf showed that the flow is subcritical hence the reduced mixing rate.

The echo sounding transects on the shelf revealed a very complex bottom bathymetry pattern. Four major canyons at the 100 m contour line are revealed which transport the Mediterranean water to the continental slope. Future experiments in this area should concentrate in this zone so as to obtain the Mediterranean properties on the continental slope.

The large scale survey was intended to observe the circulation pattern on the slope edge. ADCP measurements showed evidence of a Rossby like disturbance in the eastern flow. On the shelf where ADCP surveying was also carried out, a cyclonic circulation pattern was observed.

7

Acknowledgements

The authors wish to thank the captain and crew of the NRV *Alliance* and TCG *Cubuklu* together with the Turkish Navy Department of Navigation, Hydrography and Oceanography for their assistance in the collection of oceanographic data. Many thanks to R. Della Maggiora and A. Brogini for their efforts in preparing the oceanographic instrumentation and G. Baldasserini for carrying out the preliminary oceanographic data processing. The swath processing was carried out by A. Trangeled and C. Sisti. NOAA satellite images were prepared by E. Nacini. Special thanks to D. Farmer of the Institute of Ocean Sciences, Canada for lending us his echosounder and acoustic scintillation instruments.

References

Di Iorio, D. and Farmer, D. (1994). Path averaged turbulent dissipation measurements using high frequency acoustical scintillation analysis. *Journal Acoustical Society America*, 96:1056–1069.

Di Iorio, D. and Farmer, D. (1998). Separation of current and sound speed in the effective refractive index for a turbulent environment using reciprocal acoustic transmission. *Journal Acoustical Society America*, 103:321–329.

Di Iorio, D. and Yüce, H. (1999). Observations of Mediterranean flow into the Black Sea. *Journal Geophysical Research*, 104:3091–3108.

Farmer, D. and Denton, R. (1985). Hydraulic control of flow over the sill in Observatory Inlet. *Journal Geophysical Research*, 90:9051–9068.

Monin, A. and Ozmidov, R. (1985). *Turbulence in the Ocean.* D. Reidel, Norwell, Mass.

Oğuz, T., Özsoy, E., Latif, M., Sur, H., and Ünlüata, Ü. (1990). Modeling of hydraulically controlled exchange flow in the Bosphorus Strait. *Journal Physical Oceanography*, 20:945–965.

Oğuz, T. and Rozman, L. (1991). Characteristics of the Mediterranean underflow in the southwestern Black Sea continental shelf/slope region. *Oceanologica Acta*, 14:433–444.

Ozsoy, E., Latif, M., Besiktepe, S., Cetin, N., Gregg, M., Belokopytov, V., Goryachkin, Y., and Diaconu, V. (1997). The bosphorus strait: Exchange fluxes, currents and sea-level changes. In *NATO ARW, TU-Black Sea Results*, Sevastopol, Ukraine.

Pond, S. and Pickard, G. (1983). *Introductory Dynamical Oceanography.* Pergamon Press, 2nd edition.

Tatarskii, V. (1971). *The Effects of the Turbulent Atmosphere on Wave Propagation.* translated from Russian, by Israeli Program for Scientific Translations, Jerusalem.

Document Data Sheet

NATO UNCLASSIFIED

Security Classification		Project No.
UNCLASSIFIED		022-1
Document Serial No.	**Date of Issue**	**Total Pages**
SR-305	April 1999	59 pp.

Author(s)

Di Iorio, D., Akal, T., Guerrini, P., Yüce, Gezgin, E., Özsoy, E.

Title

Oceanographic measurements of the West Black Sea: June 15 to July 5, 1996

Abstract

An extensive survey was carried out in the Black Sea exit region of the Strait of Istanbul (Bosporus). The data described in this report builds on the knowledge learned during the Black Sea 1995 sea trial. Extensive measurements were made at the northern sill so as to describe the internal hydraulic conditions. It is shown that flow over the sill at three measurement points (south of the sill, on the sill and north of the sill) is subcritical. During the observation period the flow of Mediterranean water was continuous (i.e. no blockage events occurred as the relative sea level difference did not exceed 45 cm). The Mediterranean bottom boundary layer showed strong levels of turbulence and measurements of bottom friction coefficient range from 5 to 15 $\times 10^{-3}$.

The flow of Mediterranean water on the continental shelf is subcritical and the dilution occurs at a rate of 0.1 psu km^{-1}. Echo sounder imaging identified the major canyons which carry the effluent out to the continental slope. During the shelf survey a cyclonic circulation pattern was observed and during the deep sea survey the circulation pattern showed a general eastward direction with possibly a Rossby wave instability of approximately 70 km in wavelength. NOAA satellite infrared images could not be used to reveal such instabilities.

Keywords

Issuing Organization

North Atlantic Treaty Organization
SACLANT Undersea Research Centre
Viale San Bartolomeo 400, 19138 La Spezia, Italy

[From N. America: SACLANTCEN (New York) APO AE 09613]

Tel: +39 0187 527 361
Fax:+39 0187 524 600

E-mail: library@saclantc.nato.int

NATO UNCLASSIFIED

Initial Distribution for SR-305

Ministries of Defence

DND Canada	10
CHOD Denmark	8
MOD Germany	15
HNDGS Greece	12
MARISTAT Italy	9
MOD (Navy) Netherlands	12
NDRE Norway	10
MOD Portugal	5
MDN Spain	2
TDKK and DNHO Turkey	5
MOD UK	20
ONR USA	32

NATO Commands and Agencies

NAMILCOM	2
SACLANT	3
CINCEASTLANT/ COMNAVNORTHWEST	1
CINCIBERLANT	1
CINCWESTLANT	1
COMASWSTRIKFOR	1
COMSTRIKFLTANT	1
COMSUBACLANT	1
SACLANTREPEUR	1
SACEUR	2
CINCNORTHWEST	1
CINCSOUTH	1
COMEDCENT	1
COMMARAIRMED	1
COMNAVSOUTH	1
COMSTRIKFORSOUTH	1
COMSUBMED	1
NC3A	1
PAT	1

Scientific Committee of National Representatives

SCNR Belgium	1
SCNR Canada	1
SCNR Denmark	1
SCNR Germany	1
SCNR Greece	1
SCNR Italy	1
SCNR Netherlands	2
SCNR Norway	1
SCNR Portugal	1
SCNR Spain	1
SCNR Turkey	1
SCNR UK	1
SCNR USA	2
SECGEN Rep. SCNR	1
NAMILCOM Rep. SCNR	1

National Liaison Officers

NLO Canada	1
NLO Denmark	1
NLO Germany	1
NLO Italy	1
NLO Netherlands	1
NLO Spain	1
NLO UK	1
NLO USA	1

Sub-total	188
SACLANTCEN	30
Total	218